Plant Physiology®

Plant Physiology, 2024, 00, 1–16
https://doi.org/10.1093/plphys/kiae590
Advance access publication 10 December 2024
Research Article

Arabidopsis RNA–binding proteins interact with viral structural proteins and modify turnip yellows virus accumulation

Déborah Kiervel,[1,†] Sylvaine Boissinot,[2,3,†] Céline Piccini,[1] Danile Scheidecker,[1] Claire Villeroy,[2] David Gilmer,[1] Véronique Brault,[2,*] Véronique Ziegler-Graff[1,*]

[1]Institut de biologie moléculaire des plantes, CNRS, Université de Strasbourg, 67084 Strasbourg, France
[2]INRAE, Université de Strasbourg, SVQV UMR1131, 68000 Colmar, France
[3]INRAE, BFP UMR 1332, Université de Bordeaux, 33882 Villenave d'Ornon, France
*Author for correspondence: veronique.brault@inrae.fr (V.B.), veronique.ziegler-graff@ibmp-cnrs.unistra.fr (V.Z.-G.)
†These authors contributed equally to this work.
The author responsible for distribution of materials integral to the findings presented in this article in accordance with the policy described in the Instructions for Authors (https://academic.oup.com/plphys/pages/General-Instructions) is Véronique Ziegler-Graff. (veronique.ziegler-graff@ibmp-cnrs.unistra.fr)

Abstract

As obligate intracellular parasites, viruses depend on host proteins and pathways for their multiplication. Among these host factors, specific nuclear proteins are involved in the life cycle of some cytoplasmic replicating RNA viruses, although their role in the viral cycle remains largely unknown. The polerovirus turnip yellows virus (TuYV) encodes a major coat protein (CP) and a 74 kDa protein known as the readthrough (RT) protein. The icosahedral viral capsid is composed of the CP and a minor component RT*, arising from a C-terminal cleavage of the full-length RT. In this study, we identified Arabidopsis (*Arabidopsis thaliana*) ALY family proteins as interacting partners of TuYV structural proteins using yeast 2-hybrid assays and co-immunoprecipitations *in planta*. ALY proteins are adaptor proteins of the THO-TREX-1 complex essential to the nuclear export of mature messenger RNAs (mRNAs). Although all 4 ALY proteins colocalized with the CP and the RT protein in the nucleus upon co-expression in agro-infiltrated *Nicotiana benthamiana* leaves, only the CP remained nuclear and colocalized with ALY proteins in TuYV-infected cells, suggesting that the CP is an essential partner of ALY proteins. Importantly, TuYV-infected *A. thaliana 4xaly* knock-out mutants showed a significant increase in viral accumulation, indicating that TuYV infection is affected by an unknown ALY-mediated antiviral defense mechanism or impairs the cellular mRNA export pathway to favor viral RNA translation. This finding underpins the crucial role played by nuclear factors in the life cycle of cytoplasmic RNA viruses.

Introduction

Plant viruses have small and compact genomes encoding a reduced number of proteins. To circumvent their small coding capacity, they rely on host factors to fulfill their infectious cycle. They also evolved to overcome antiviral defenses such as post-transcriptional gene silencing and autophagy by encoding various defense suppressors (Kushwaha et al. 2019; Wu et al. 2019; Jin et al. 2022). Host–virus interactions are therefore crucial for successful viral replication and propagation in the plant. Identification of these interactions is of practical interest since host proteins can be the target of genetic breeding programs to identify resistance genes (Dodds and Rathjen 2010; Nicaise 2015; Garcia-Ruiz 2018).

In metazoans, the nuclear export of messenger RNAs (mRNAs) is a complex process central to gene expression that involves the participation of numerous proteins that viruses can harness to manipulate cellular processes (Tessier et al. 2019). mRNA nucleo-cytoplasmic export occurs during their biogenesis and maturation (splicing, capping, and polyadenylation) through the recruitment of RNA-binding proteins that serve as platforms recognized by the heterodimeric export factors TAP/p15 (also known as NXF1/NXT1 in metazoans and Mex67/Mtr2 in yeast) (Kang and Cullen 1999; Stewart 2019). To date, such export factors remain unknown in plants (Ehrnsberger et al. 2019). The role of the coordinator between transcription, maturation, and export of mRNAs is provided by the TRanscription-EXport complex 1 (TREX-1) (Heath et al. 2016). TREX-1 is a multiproteic complex composed of a THO protein core, the UAP56 RNA helicase, the CIP29 protein, and the adaptor protein ALY (also called ALY/REF or REF in metazoans or Yra1 in yeast) (Masuda et al. 2005; Chi et al. 2013). After the recruitment of these proteins on the nascent RNAs undergoing maturation, the THO complex and the ALY protein allow the mobilization of TAP/p15 factors, which then ensure mRNA guidance toward the nuclear pores from where they will be transported to the cytoplasm (Viphakone et al. 2012).

Many studies have highlighted the importance of the TREX complex in the export of a wide range of viral mRNAs encoded by DNA viruses that are transcribed in the nucleus (Gales et al. 2020). For instance, the ICP27 protein of herpes simplex virus 1

Received May 6, 2024. Accepted October 1, 2024.
© The Author(s) 2024. Published by Oxford University Press on behalf of American Society of Plant Biologists.
This is an Open Access article distributed under the terms of the Creative Commons Attribution-NonCommercial-NoDerivs licence (https://creativecommons.org/licenses/by-nc-nd/4.0/), which permits non-commercial reproduction and distribution of the work, in any medium, provided the original work is not altered or transformed in any way, and that the work is properly cited. For commercial re-use, please contact reprints@oup.com for reprints and translation rights for reprints. All other permissions can be obtained through our RightsLink service via the Permissions link on the article page on our site—for further information please contact journals.permissions@oup.com.

Downloaded from https://academic.oup.com/plphys/advance-article/doi/10.1093/plphys/kiae590/7920476 by guest on 12 December 2024

promotes the nuclear export of viral RNAs *via* its interactions with viral mRNAs, the ALY protein, and TAP export factors (Tian et al. 2013). More recently, the interaction between hepatitis B virus (HBV) HBx protein and TREX helicase protein UAP56 was shown to play a central role in the nuclear export of HBV transcripts (Hu et al. 2020). Among plant viruses, the first description of a viral RNA export mediated by the TREX complex is the pregenomic 35S RNA of cauliflower mosaic virus (CaMV) (Kubina et al. 2021). The export of this polycistronic viral RNA involves numerous protein partners, among which ALY proteins play a prominent role (Ehrnsberger et al. 2019). More surprisingly, RNA viruses also express proteins able to interact with TREX complex factors (Park et al. 2004; Canto et al. 2006; Maio et al. 2020; Yang et al. 2020).

Although the vast majority of RNA viruses replicate in the cytoplasm, many of them express viral proteins that display a nuclear localization (Brice et al. 2021; Rodriguez-Peña et al. 2021). Such a localization can be associated with the redistribution of host nuclear proteins to the cytoplasm to promote the translation or replication of RNA viruses or even a systemic movement in the case of plant viruses. Picornaviruses, for instance, can destabilize the nuclear pore complexes, resulting in a massive disruption of the nucleocytoplasmic transport of RNAs and proteins in infected cells (Lizcano-Perret and Michiels 2021). Such disruption leads to the retention of polyadenylated mRNAs in the nucleus, thus preventing the translation of mRNA coding for antiviral proteins and allocating the translational machinery to the virus. In addition, viral proteins can also target the nucleus to inhibit nuclear functions or suppress innate immunity signaling by the cytoplasmic retention of transcription-activation factors (Lizcano-Perret and Michiels 2021).

Among plant RNA viruses that encode proteins with nuclear localization, the potato leafroll virus (PLRV) encodes a coat protein (CP) targeting the nucleolus (Haupt et al. 2005). The PLRV is the type member of the *Polerovirus* genus belonging to the recently assigned *Solemoviridae* family. These viruses infect plants from a wide range of families (from *Poaceae* to *Solanaceae*, *Brassicaceae*, *Cucurbitaceae*, *Amaranthaceae*) and are responsible for causing substantial economic damage to important crops (Edwards et al. 2001; D'Arcy and Domier 2005a; Jones et al. 2007; Hossain et al. 2021). Poleroviruses are restricted to phloem cells and are strictly transmitted by aphids in a circulative and nonpropagative manner D'Arcy and Domier 2005b.

The polerovirus genome is linked to a viral genome–binding protein at its 5′ extremity and contains 7 to 9 open reading frames (Delfosse et al. 2021). The viral RNA is protected by a nonenveloped icosahedral capsid of 25 nm in diameter composed of 2 proteins: the major CP translated from ORF3 and the minor CP RT*. RT* is a C-terminal truncated version of the readthrough (RT) protein translated from ORF3 and ORF5 by a stop codon suppression mechanism, but the exact C-terminal amino acid has not been yet determined (Revollon et al. 2010). In addition to their structural features, both the CP and the RT* protein are required for efficient viral systemic movement *in planta* and for virus transmission by aphids (Brault et al. 1995; Bruyère et al. 1997; Mutterer et al. 1999; Peter et al. 2008; Boissinot et al. 2014). Moreover, virion formation has been reported to be essential for long distance movement of turnip yellows virus (TuYV) in Arabidopsis (*Arabidopsis thaliana*) (Hipper et al. 2014). The RT domain (downstream of the CP sequence) contains a highly conserved N-terminal part and a C-terminal domain (RT_{Cter}) with a high sequence variability among poleroviruses. The RT_{Cter} influences symptom development associated with infection (Bruyère et al. 1997; Peter et al. 2008) and virus long-distance trafficking in a host-dependent manner (Rodriguez-Medina et al. 2015). Peter et al. (2009) also reported that the RT_{Cter} of the PLRV regulates virus restriction to phloem tissue.

In a former yeast 2-hybrid screen of an aphid *Myzus persicae* cDNA library, the TuYV structural proteins CP and $RT_{\Delta Cter}$ (the size of which is close to the natural RT* and is akin to the structural protein, Rodriguez-Medina et al. 2015) were found to interact with ALY, ortholog of the aphid *Acyrthosiphon pisum* encoded protein (accession number ACYPI006176-RA, Mulot et al. 2016). Attempts to silence the expression of the unique ALY gene in *M. persicae* by RNA interference remained ineffective, thus preventing a functional analysis of this protein in aphids (Mulot et al. 2016). Nevertheless, recent unpublished data of affinity purification experiments coupled to mass spectrometry performed with a tag-labeled RT protein stably expressed in Arabidopsis plants identified host plant ALY proteins as interacting partners of the viral protein (D. Kiervel and V. Ziegler-Graff, IBMP Strasbourg). *A. thaliana* encodes 4 ALY proteins (ALY1 to ALY4, with respective molecular weights of 25.8, 30.8, 31.3, 30.4 kDa), which play a role in the mRNA nuclear export pathway and modulate plant growth and development (Pfaff et al. 2018).

In this study, we investigated the interaction between the 4 nuclear ALY proteins from *A. thaliana* and TuYV structural proteins. We showed by yeast 2-hybrid assays and co-immunoprecipitation experiments *in planta* that ALY proteins interact in vivo with the TuYV CP and the RT protein. We further investigated the colocalization of both ALY and viral proteins when expressed ectopically or together with the virus in *Nicotiana benthamiana* leaves. Importantly, we demonstrated that the inhibition of ALY gene expression in an *A. thaliana* quadruple mutant significantly enhanced TuYV accumulation, suggesting either an antiviral function of ALY proteins or an indirect proviral effect of ALY diversion through their interaction with TuYV structural proteins, thus leading to a decrease of cellular mRNA export.

Results

CP and the $RT_{\Delta Cter}$ protein interact with *A. thaliana* ALY proteins in yeast

We first investigated the interaction of the 4 *Arabidopsis* ALY proteins with the TuYV CP and the RT protein by yeast 2-hybrid experiments. ALY1-4 protein sequences were expressed as fusions to the activation domain of GAL4 transcription factor. As both the full-length and the N-terminal part of the RT domain (RT_{Nter}) fused to the binding domain of GAL4 showed an autoactivation of the reporter gene (Rodriguez-Medina et al. 2015), their interaction with ALY proteins could not be addressed. TuYV structural protein sequences (the CP and $RT_{\Delta Cter}$), and the C-terminal domain of the RT protein sequence (RT_{Cter}), were fused to the GAL4 DNA binding domain. Interactions between ALY proteins and the viral proteins were analyzed by plating 3 double-transformed yeast colonies on an SD/-WL medium and on the interaction-selective medium supplemented with the aureobasidin A antibiotic (SD/-AHWL + Aur). The absence of transcription autoactivation activity of the reporter genes by the individual viral or ALY proteins was controlled (Supplementary Fig. S1).

After 4 d of yeast growth on SD/-AHWL + Aur, ALY1 and ALY3 were shown to strongly interact with the CP and $RT_{\Delta Cter}$ (Fig. 1), whereas no interaction between the ALY2, ALY4, and CP or $RT_{\Delta Cter}$ proteins was clearly observed (Fig. 1A). However, in an additional experiment, we observed that a few colonies co-transformed with ALY2 or ALY4 and the $RT_{\Delta Cter}$ developed on a selective medium, suggesting a weak interaction between ALY2 or ALY4 and the viral protein (Fig. 1B). It could be concluded that ALY1 and

Downloaded from https://academic.oup.com/plphys/advance-article/doi/10.1093/plphys/kiae590/7920476 by guest on 12 December 2024

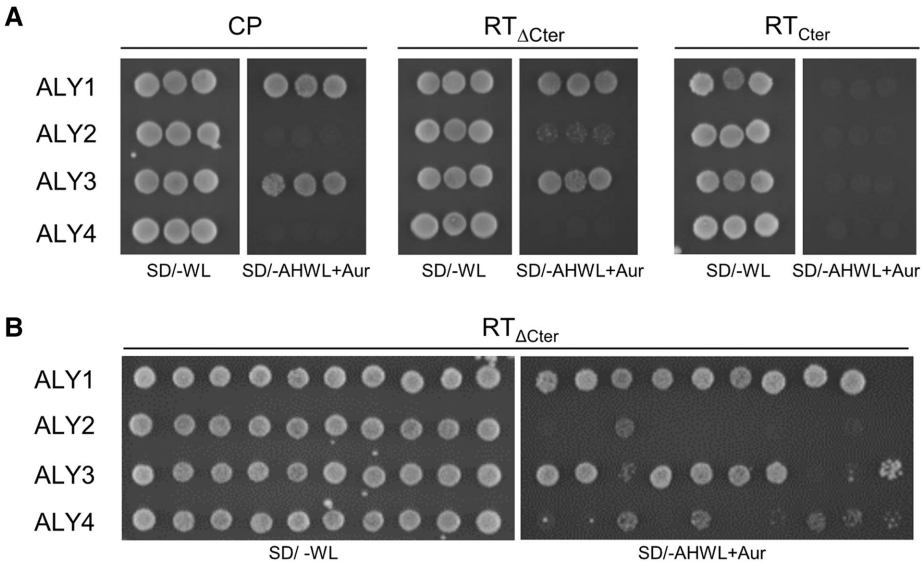

Figure 1. Yeast 2-hybrid interaction tests between *A. thaliana* ALY proteins (ALY1-4) and TuYV proteins (CP and $RT_{\Delta Cter}$) or the RT_{Cter} domain. **A)** Yeast cells were co-transformed with recombinant plasmids expressing an ALY protein (pGADT7) or a viral protein (pGBKT7) and selected on a minimum medium lacking tryptophan and leucine (SD/-WL). Interaction tests were performed on a minimum media lacking adenine, histidine, tryptophan, and leucine and supplemented with aureobasidin A antibiotic (SD/-AHWL + Aur). Three colonies were plated for each modality. **B)** An independent experiment examining the interaction between ALY and $RT_{\Delta Cter}$ was performed with 10 yeast colonies plated on SD/-WL and on SD/-AHWL + Aur.

ALY3 interacted with the CP and $RT_{\Delta Cter}$, whereas ALY2 or ALY4 could bind the $RT_{\Delta Cter}$ but at a low efficiency. Interestingly, no interaction occurred between any ALY protein and the RT_{Cter}, highlighting the absence of involvement of this domain in interactions with the ALY proteins. In contrast, considering that the $RT_{\Delta Cter}$ contains the CP at its N-terminus and that both the CP and the $RT_{\Delta Cter}$ protein share the same interaction profile with ALY1 and ALY3, it is likely that in yeast, the $RT_{\Delta Cter}$ protein interaction with these ALY proteins occurs through the CP domain.

The TuYV CP and the RT protein co-immunoprecipitate with ALY proteins *in planta*

To further evaluate the in vivo interaction of ALY proteins with the TuYV CP and the RT protein, we performed co-immunoprecipitation experiments on agro-infiltrated *N. benthamiana* plants. Because the RT^* protein is detected only in viral particles and not in plant extracts (Filichkin et al. 1994; Brault et al. 1995), we carried out the experiment with the full-length RT protein. *N. benthamiana* leaves were co-infiltrated with *Agrobacterium tumefaciens* expressing either the CP or the RT protein, 1 of the 4 GFP-tagged ALY proteins, and the appropriate viral suppressor of silencing (VSR) to improve protein expression (see Supplementary Fig. S2 and the Materials and methods section for VSR selection). Note that ALY3:GFP was weakly detected in any condition possibly due to protein instability (Supplementary Fig. S2C). ALY:GFP immunoprecipitation (IP) performed with cell lysates from 4-d postinfiltrated (pi) leaves pulled down the CP and the RT protein, indicating that *in planta*, both viral proteins interacted with any of the 4 ALY:GFP proteins without the requirement of any other viral factors (Fig. 2, A and B). Neither the CP nor the RT protein co-immunoprecipitated with the GFP control, highlighting the specificity of interaction between the viral proteins and the ALY proteins (Fig. 2, A and C, IP).

This experiment was also carried out with ALY:GFP proteins co-expressed in infected leaves. In these conditions also, both the CP and the RT protein were co-immunoprecipitated with all 4 ALY proteins (Supplementary Fig. S3), suggesting that neither the viral genome nor other viral proteins prevented this interaction.

ALY proteins colocalize with both the TuYV CP and the RT protein in *N. benthamiana*

Next, we investigated the subcellular localization of tagged ALY proteins alone or in the presence of viral structural proteins. *N. benthamiana* leaves were agro-infiltrated with plasmids expressing ALY proteins in fusion with enhanced GFP (EGFP) to optimize their detection by laser scanning confocal microscopy (LSCM). All 4 ALY:EGFP proteins were strictly detected in the nucleus (Supplementary Fig. S4), which is in agreement with what is reported in former studies (Uhrig et al. 2004; Pfaff et al. 2018). The ALY1:EGFP and ALY2:EGFP proteins were predominantly detected in numerous nucleoplasmic speckles (Supplementary Fig. S4, A and B), while ALY3:EGFP displayed a major and strong nucleolar localization (Supplementary Fig. S4C). With regard to ALY4:EGFP, a few and tiny foci were observed in the nucleoplasm and in a ring-shaped structure at the nucleolar periphery (Supplementary Fig. S4D).

We then analyzed the localization of the viral proteins fused to RFP. A transient expression of the TuYV RFP:CP alone in *N. benthamiana* leaves showed strong fluorescence within the nucleus, with a major targeting to the nucleolus (Fig. 3A). Haupt et al. (2005) reported a similar localization for the PLRV CP due to a specific nucleolar localization signal (NoLS). Surprisingly, the strong nucleolar localization of the RFP:CP was not observed for the CP:RFP, which remained essentially in the nucleoplasm (Supplementary Fig. S5A), suggesting that N- or C-terminal orientation of the fluorescent tag fused to the TuYV CP influenced the localization of the fusion protein.

When the RFP:CP or the CP:RFP was co-expressed with the ALY:EGFP proteins, both viral and cellular proteins colocalized in the nucleus. ALY1:EGFP, ALY2:EGFP, and to a lesser extent ALY4:EGFP, co-localized in discrete speckles in the nucleoplasm with both the RFP:CP (Fig. 3, B, C and E) and the CP:RFP (Supplementary Fig. S5, B, C and E), while ALY3:EGFP fluorescence was particularly intense in the nucleolus with the RFP:CP (Fig. 3D) and also around the nucleolus with the CP:RFP (Supplementary Fig. S5D).

Because the RT protein contains the CP domain at its N-terminus, we expected that the CP's NoLS motif would target

Downloaded from https://academic.oup.com/plphys/advance-article/doi/10.1093/plphys/kiae590/7920476 by guest on 12 December 2024

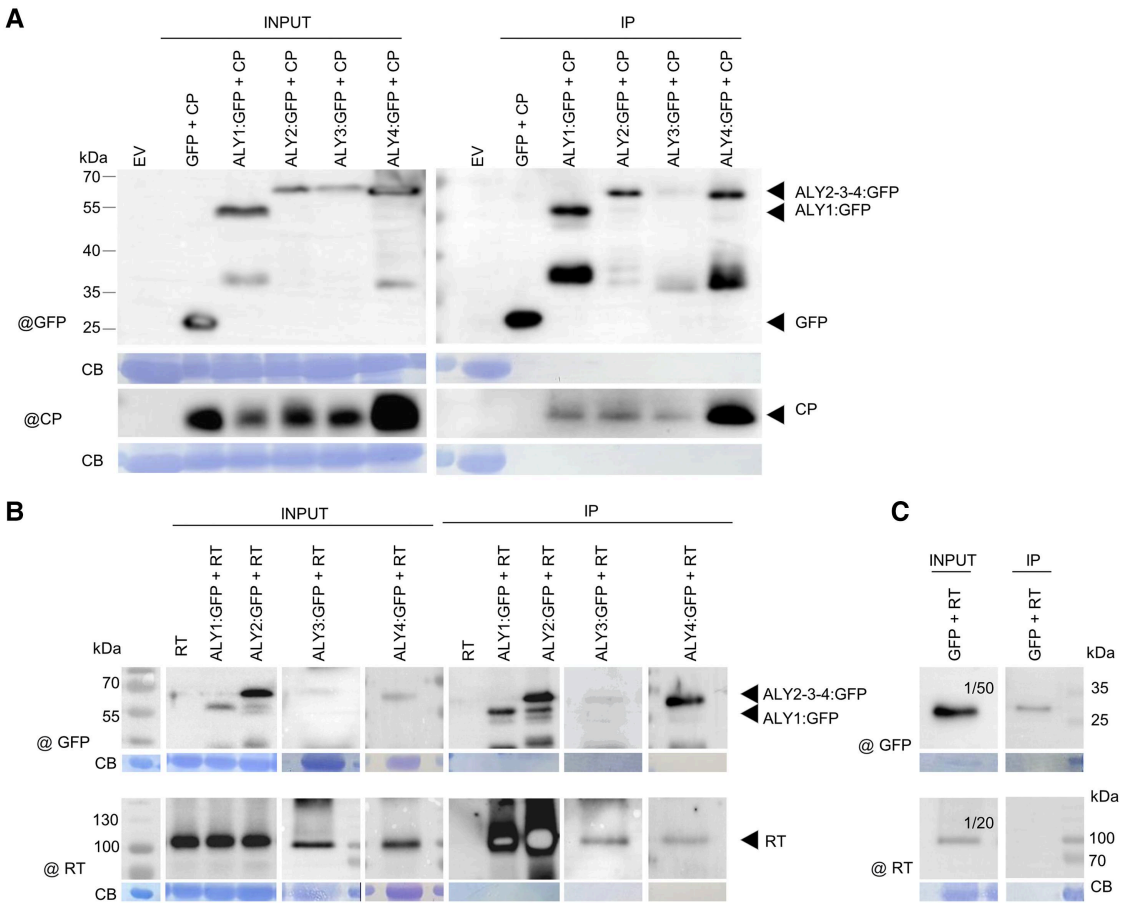

Figure 2. Interaction assays of TuYV CP and RT proteins *in planta* with each of the 4 ALY:GFP proteins. Cell lysates from 4 d post agro-infiltrated *N. benthamiana* leaves were added to beads coupled to anti-GFP antibodies to immunoprecipitate ALY:GFP and test interactions with the CP **A)** and RT **B)** protein. Input samples (INPUT) are shown in the left panels and IP samples in the right panels. Proteins were detected by western blot using anti-GFP (@GFP), anti-CP (@CP), or anti-RT (@RT) antibodies. The control for experiment **B)** is presented in **C)**. In this panel, the sample loading was reduced (1/50 and 1/20 dilution). Protein loadings were controlled by membrane staining with Coomassie blue. EV, empty vector.

the RT protein to the nucleolus. We indeed observed a nucleolar targeting of the RFP:RT protein when co-expressed with a suppressor of RNA silencing (Fig. 4A, blue arrow), but also a localization in discrete foci along the peripheral plasma membrane (Fig. 4A, white arrows). When co-expressed with the ALY:EGFP proteins, the localization patterns of the RFP:RT protein were similar to those observed with the RFP:CP, i.e. a major nucleoplasmic colocalization in various speckles described above for ALY-EGFP proteins and also to the nucleolus for ALY3-EGFP (Fig. 4, B to E). Intriguingly, the plasma membrane localization of the RFP:RT protein was lost, possibly due to a clear decrease in the expression of the viral protein when co-expressed with any of the ALY proteins, compared with the control without the ALY proteins (see Supplementary Fig. S6C, compare in the lower panel the RFP-RT band in the empty vector sample with those containing one of the ALY proteins). The expression of all fusion proteins was confirmed by a western blot analysis (Supplementary Fig. S6, A to C).

Localization of ALY proteins upon co-expression with a labeled TuYV

The subcellular localization of a host protein can be modified through its interactions with viral protein partners (Rodriguez-Peña et al. 2021). In order to analyze the fate of ALY:EGFP localization during viral infection, we constructed a TuYV clone expressing the RT protein in fusion with a TagRFP label (tRFP). According to the cloning strategy previously used to produce the TuYV-RT_{GFP} infectious clone (Boissinot et al. 2017), we replaced 174 amino acids at the C-terminus of the RT protein by the tRFP (Fig. 5A). Two versions of the RT protein were generated (Fig. 5A). In the TuYV-$RT_{\Delta Cter}$:$tRFP_{fus}$ mutant, the genuine last 8 amino acids of the RT protein were maintained in the frame downstream of the inserted tRFP sequence, while in TuYV-$RT_{\Delta Cter}$:$tRFP_{stop}$, the fusion protein ended with the fluorescent protein. Both viral clones were introduced into a binary vector and agro-inoculated into *N. benthamiana* leaves. Three days post infiltration, the expression of the CP and RT fusion proteins was detected in infiltrated leaves by western blot using specific antibodies. The CP was clearly detected for all viral constructs (Fig. 5B). The wild-type RT migrated with an apparent molecular weight of 95 kDa, as previously reported (Boissinot et al. 2017), and the fused $RT_{\Delta Cter}$-tRFP proteins showed similar apparent molecular weight, as expected, due to the replacement of the C-terminal domain of the RT protein by the tRFP (Fig. 5, A and B). We then assessed the capacity of both viral clones to systemically infect plants by measuring the viral titer by ELISA in noninoculated leaves. Reduced infection rates and virus accumulations were observed for both recombinant viruses when compared with $TuYV_{WT}$ (Supplementary Table S1). However, no significant differences were found between the mutated viruses (TuYV-$RT_{\Delta Cter}$:$tRFP_{fus}$ and TuYV-$RT_{\Delta Cter}$:$tRFP_{stop}$),

Downloaded from https://academic.oup.com/plphys/advance-article/doi/10.1093/plphys/kiae590/7920476 by guest on 12 December 2024

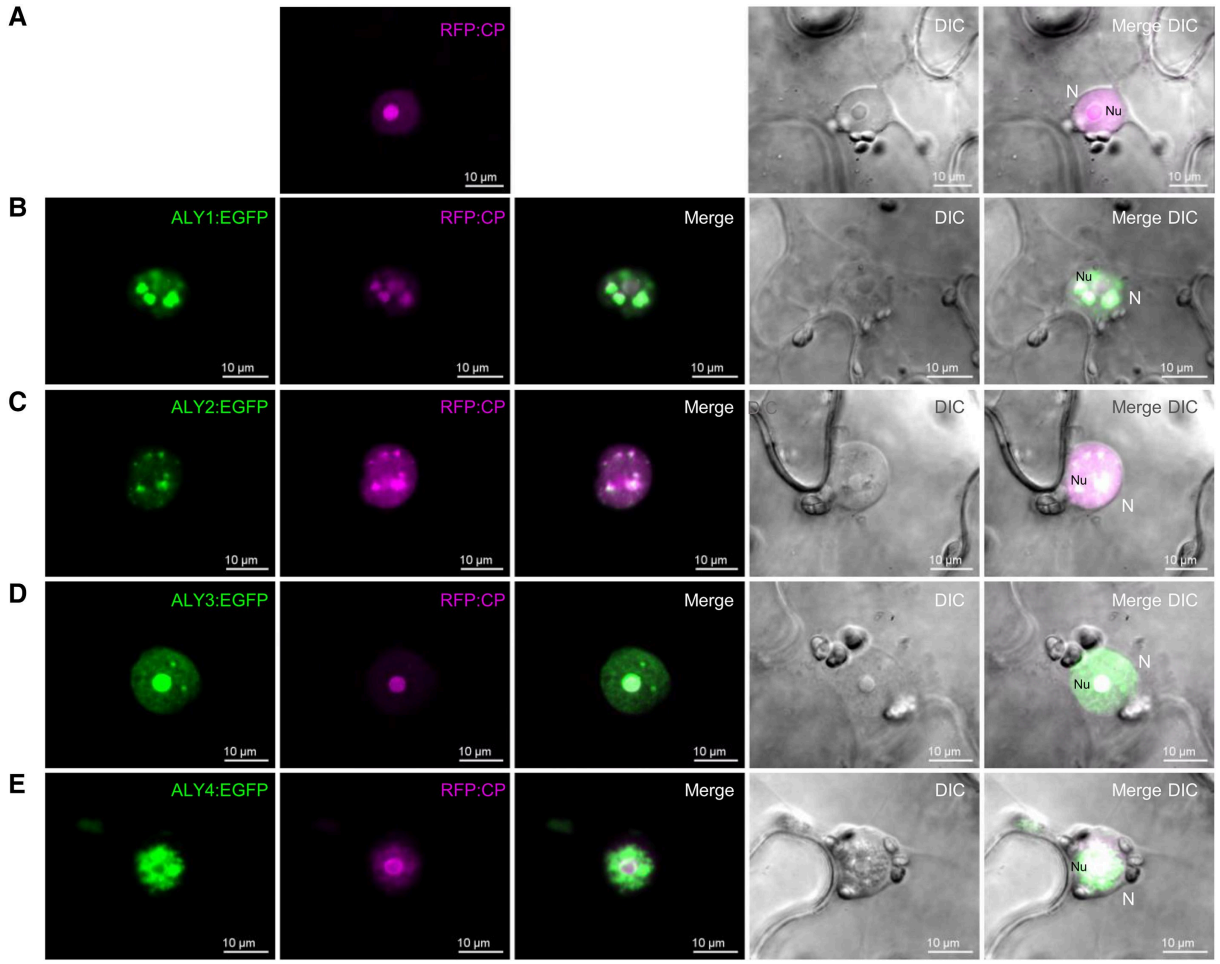

Figure 3. Subcellular colocalization analysis of ALY:EGFP and TuYV CP proteins. *N. benthamiana* leaf tissues expressing RFP:CP alone **A)** or in co-expression with ALY1:EGFP to ALY4:EGFP **B** to **E)** were analyzed 3 d post infiltration by LSCM. EGFP and RFP channels are presented in the first and second columns, respectively, and the merging of the two in the central column. DIC and the merging of all channels (Merge DIC) are shown in the fourth column and last column. $n = 2$, 4 leaf disks cut out in 2 or 3 leaves/plants, and 4 to 22 regions of interest (ROIs) were analyzed/experimented. Scale bars: 10 µm. N, nucleus; Nu, nucleolus.

indicating that the last 8 amino acids at the C-terminus of the RT protein (absent as a coding sequence in TuYV-RT$_{\Delta Cter}$:tRFP$_{stop}$) were not sufficient to recover the viral accumulation level lost by the deletion of the C-terminal domain. We controlled the stability of the tRFP sequence introduced in the TuYV genome by analyzing the viral progeny in noninoculated leaves by an RT-PCR of plants infected with either recombinant virus. The presence of a major band of the expected size indicated that the tRFP sequence inserted into the TuYV genome was conserved in the viral progenies present in systemically infected leaves (Supplementary Fig. S7A).

We further examined systemic tissues infected with the tagged viruses by epifluorescence microscopy and detected discrete red punctuations in the phloem cells of *N. benthamiana* petioles and roots, confirming that both recombinant TuYV viruses moved over long distances and still expressed the tRFP label (Supplementary Fig. S7B). Phloem restriction was also retained. Finally, we investigated the subcellular localization of the fused RT:tRFP proteins 3 d post infiltration in *N. benthamiana* leaves by LSCM. Both TuYV-RT$_{\Delta Cter}$:tRFP$_{fus}$ and TuYV-RT$_{\Delta Cter}$:tRFP$_{stop}$ mutants induced the formation of large cytoplasmic structures next to the nucleus, partially labeled with tRFP, which will be referred thereafter as perinuclear aggregates (Fig. 5C). These structures were specific to TuYV infection, and co-expression with EGFP did not affect their presence [Supplementary Fig. S8A, see differential interference contrast (DIC) panel, surrounded by a dotted line]. In contrast to RFP:RT expressed ectopically (Fig. 4A), the RT$_{\Delta Cter}$:tRFP expressed by the modified viruses was absent from the nucleus and the plasma membrane but was essentially detected in the perinuclear aggregates (Fig. 5C). This suggests that the RT$_{Cter}$ domain (absent in the RT$_{\Delta Cter}$ protein) may be responsible for the targeting to the plasma membrane of the entire RT protein (see more examples in Fig. 6, A to D). Similarly, *A. thaliana* protoplasts infected with the tagged viruses and analyzed 24 h post transfection showed the formation of cytoplasmic aggregates labeled with RT:tRFP (Supplementary Fig. S7C), which were absent in cells transfected with EGFP alone (Supplementary Fig. S7D).

Next, we investigated the localization of the ALY:EGFP when co-expressed with TuYV-RT$_{\Delta Cter}$:tRFP$_{fus}$, which will be referred to as the TuYV-RT$_{\Delta Cter}$:tRFP in the following experiments. As shown in Fig. 6, A to D, all ALY proteins (ALY1:EGFP to ALY4:EGFP) conserved their nuclear distribution, while the RT$_{\Delta Cter}$:tRFP was targeted to large perinuclear aggregates. We did not observe any colocalization between the ALY and the RT proteins, except in a few cases where we noticed that the ALY3:EGFP and ALY4:EGFP co-localized faintly with the RT protein in the cytoplasmic viral-induced structures (Fig. 6, C and D, white arrows). Such

Downloaded from https://academic.oup.com/plphys/advance-article/doi/10.1093/plphys/kiae590/7920476 by guest on 12 December 2024

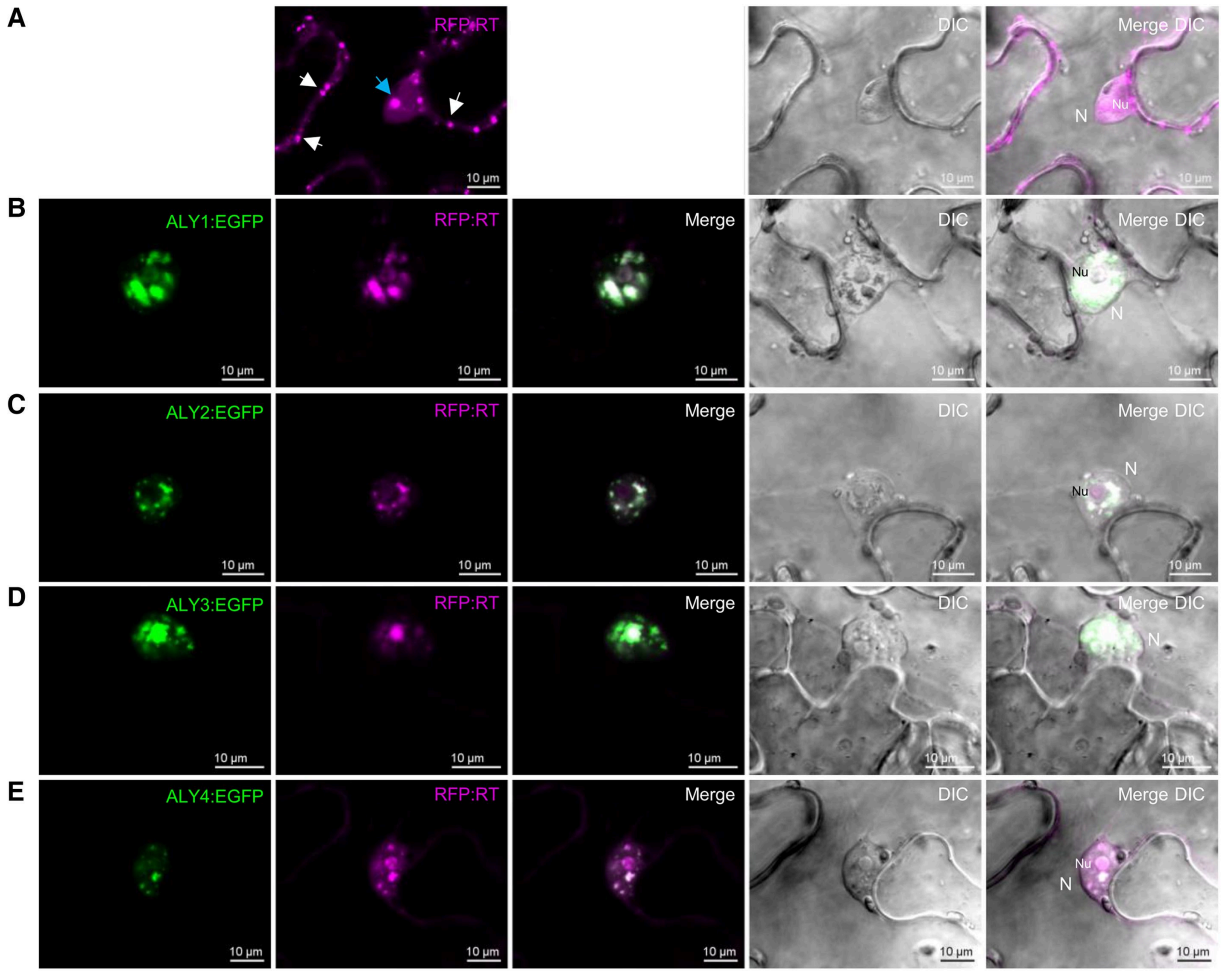

Figure 4. Subcellular colocalization analysis of ALY:EGFP and TuYV RT proteins. Three days post infiltration, *N. benthamiana* leaf tissues expressing RFP:RT and VSR P38 **A)** or in co-expression of the 2 former constructs with ALY1:EGFP to ALY4:EGFP **B** to **E)** were analyzed by LSCM. EGFP or RFP channels are presented in the first and second columns, respectively, and the merger in the central column. DIC and the merger of all channels (Merged DIC) are shown in the fourth column and last column. The white arrows in A indicate the membrane localization of the RFP:RT protein and the blue arrow points its localization in the nucleolus. $n = 2$, 4 leaf disks cut out in 2 or 3 leaves/plants, and 6 to 17 ROIs were analyzed/experimented. Scale bars: 10 µm. N, nucleus; Nu, nucleolus.

distribution may possibly result from some partial nuclear envelope disruption. We also examined the localization of the ALY proteins in the presence of the major CP upon viral infection. As the CP could not be fused to a fluorescent tag in the viral genome without generating translation issues with the other ORFs expressed by the subgenomic RNA, we observed that the ALY proteins in *N. benthamiana* leaves co-infiltrated with the RFP:CP and $TuYV_{WT}$ (Fig. 6, E to H). In these conditions, the fluorescent CP colocalized with the ALY proteins in speckles of different sizes in the nucleus and formed punctuated foci in the viral-induced structures (identifiable with DIC) and along the plasma membrane (Fig. 6, E to H). The nucleoli were also markedly dual-labeled by the RFP:CP and ALY1, ALY3, and ALY4 (Fig. 6, E, G and H). Interestingly, when the CP:EGFP or EGFP:CP was co-expressed with the TuYV-$RT_{\Delta Cter}$:tRFP, the CP colocalized with the $RT_{\Delta Cter}$:tRFP in a more diffuse way in the perinuclear aggregates (Supplementary Fig. S9, C and D). Due to CP colocalization with each ALY protein in infected cells, it may suggest that the CP would be the major interactant of these host proteins during infection. The expression of the fusion proteins was controlled by western blot for all infiltration experiments (Supplementary Fig. S6, D and E).

TuYV accumulation increases in an *A. thaliana 4xaly* quadruple mutant

Finally, to analyze the biological relevance of these interactions and colocalizations in the viral infection process, we first tested the potential influence of TuYV infection on the expression of *ALY* genes by measuring *ALY1* to *ALY4* mRNA accumulation in TuYV-infected Col-0 plants (Supplementary Fig. S10). No statistically significant differences in *ALY* mRNA accumulation were observed for any of the 4 ALY proteins when comparing accumulation in TuYV-systemically infected or mock-inoculated *Arabidopsis* plants. We then enquired whether the absence of 1 *ALY* gene could affect TuYV systemic infection by inoculating single knock-out (KO) mutants with viruliferous aphids and found no major changes in the viral titer (Supplementary Table S2). As the involvement of the ALY proteins in the TuYV cycle could be masked by functional redundancy in single KO mutants, we tested the susceptibility of a quadruple KO mutant (*4xaly*) to TuYV infection (Pfaff et al. 2018). In 2 independent experiments, TuYV accumulation measured by RT-qPCR increased significantly in the *4xaly* mutant by a factor of 2 and 3.3, respectively, for Experiments 1 and 2, with similar infection rates in both the

Downloaded from https://academic.oup.com/plphys/advance-article/doi/10.1093/plphys/kiae590/7920476 by guest on 12 December 2024

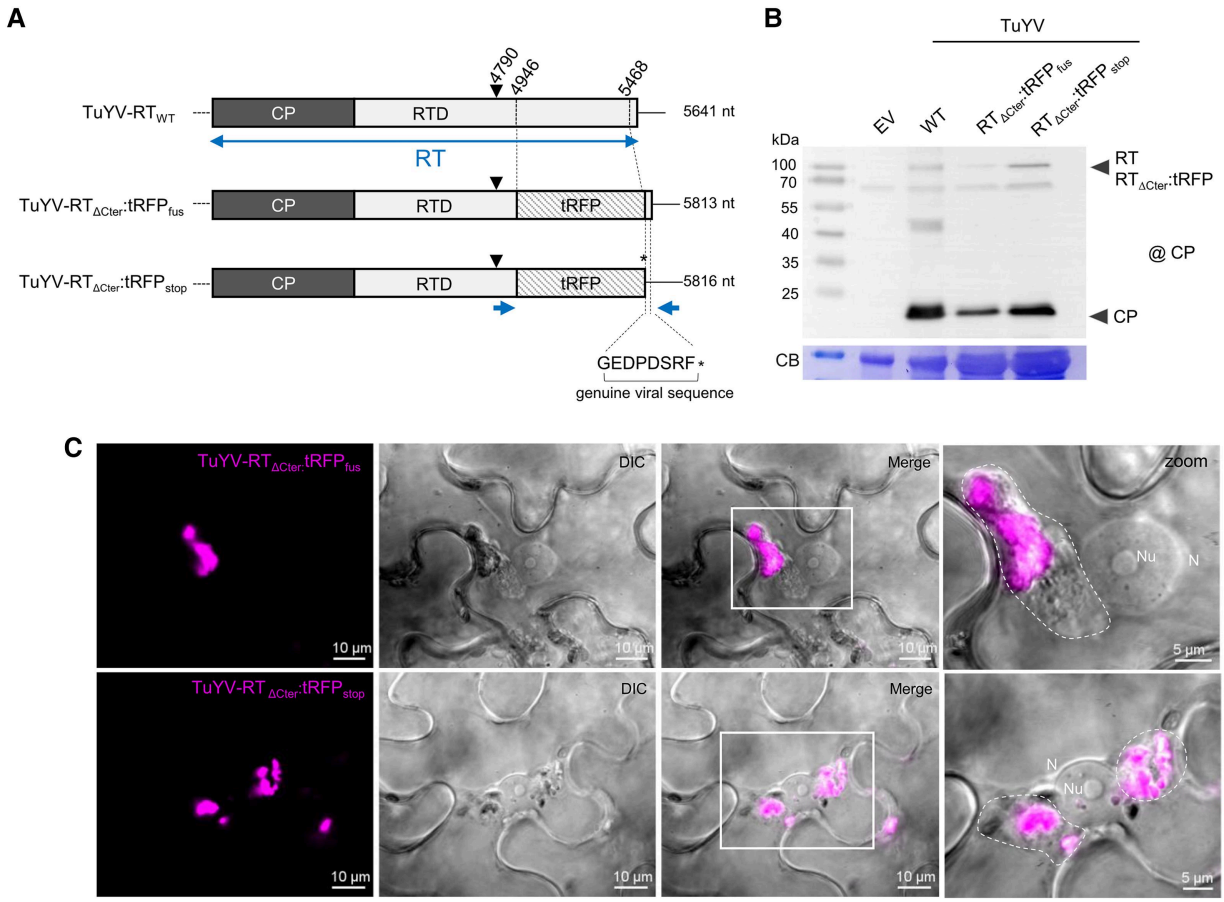

Figure 5. Map of the structural proteins encoded by TuYV$_{WT}$ and 2 tRFP recombinant TuYV clones and analysis of their infectivity in agro-inoculated leaves of *N. benthamiana*. **A)** Schematic representation of the 3′ end of the TuYV$_{WT}$ and TuYV-RT$_{\Delta Cter}$:tRFP$_{(fus)\ and\ (stop)}$ genomes. The position of the deleted sequence (nt 4,946 to 5,468) is shown on the TuYV-RT$_{WT}$ map. In TuYV-RT$_{\Delta Cter}$:tRFP$_{fus}$, the last 8 amino acids of the RT protein (mentioned below the constructs) are in fusion with the C-terminus of the tRFP. In TuYV-RT$_{\Delta Cter}$:tRFP$_{stop}$, an asterisk (*) indicates the stop codon at the end of the tRFP sequence. The length of each viral genome is mentioned. RT, readthrough protein; RTD, readthrough domain; tRFP, tag red fluorescent protein; ▼, the position of lysine K437 (nt 4,790), the last amino acid identified in the RT* protein incorporated into the virus particles. The small blue arrows below the genomes indicate the position of the primers used for progeny analysis by RT-PCR. **B)** CP and RT protein expression by TuYV-RT$_{\Delta Cter}$:tRFP$_{fus}$ and TuYV-RT$_{\Delta Cter}$:tRFP$_{stop}$ in agro-infiltrated leaves. Protein detection was performed by western blot using specific antibodies against the CP (@CP). EV, empty vector; CB, Coomassie blue membrane staining. **C)** Subcellular localization of the RT$_{\Delta Cter}$:tRFP proteins observed by LSCM in leaves agro-infiltrated with TuYV-RT$_{\Delta Cter}$:tRFP$_{fus}$ and TuYV-RT$_{\Delta Cter}$:tRFP$_{stop}$. The tRFP channel is shown on the left followed by the DIC and the merger. Perinuclear aggregates are indicated by dotted circles in the right panel (enlargements of the insets). $n = 2$, 4 leaf disks cut out in 2 or 3 leaves/plants, and 5 to 18 ROIs were analyzed/experimented. N, nucleus.

Col-0 controls (79% and 100% of infected plants) and the 4*xaly* KO mutants (93% and 92% of infected plants) (Fig. 7). These results suggest that the 4 ALY proteins may display a potential cooperative and/or redundant function in defense against TuYV infection.

Discussion

TuYV structural proteins interact with ALY proteins

In this work, we identified the *A. thaliana* ALY nuclear export adapters as interactors of TuYV structural proteins. These interactions were first established in yeast 2-hybrid assays, where ALY1 and ALY3 proteins interacted strongly with the major capsid protein CP and the related minor capsid protein RT$_{\Delta Cter}$. Noteworthy, the Cter domain of the RT protein did not interact with any of the ALY proteins. The fact that both the CP and the RT$_{\Delta Cter}$ share similar interaction profiles with ALY1 and ALY3 suggests that at least in yeast, the CP domain of the RT protein could be the domain involved in this interaction. Conversely, ALY2 and ALY4 showed a much weaker interaction with the RT$_{\Delta Cter}$ protein.

The situation was different when ALY proteins were expressed ectopically in *N. benthamiana* epidermal cells with either viral protein. All 4 ALY proteins were capable of interacting with both CP and RT proteins. Such distinct binding patterns in yeast and plant cells could reflect either a potential misfolding of the fused proteins in yeast or the absence of a plant-specific cofactor required for the interaction between the viral proteins and ALY2 or ALY4. The results obtained in plants indicate that the interaction does not require any additional viral partner. The interaction was also confirmed in infected *N. benthamiana* leaves, highlighting the fact that the expression of other viral factors does not impair the binding between viral and ALY proteins.

When transiently expressed in *N. benthamiana* leaves, both RFP:CP and RFP:RT proteins displayed a strong nucleolar localization. Such subcellular targeting was previously reported for the PLRV CP and the RT protein and was attributed to a nucleolar localization motif (NoLS) located at the N-terminus of the CP (Haupt et al. 2005). Both TuYV CP and RT proteins contain a similar arginine-rich domain near the N-terminal extremity, which is likely responsible for their nucleolar localization of both TuYV proteins when ectopically expressed in *N. benthamiana* plants. In

Downloaded from https://academic.oup.com/plphys/advance-article/doi/10.1093/plphys/kiae590/7920476 by guest on 12 December 2024

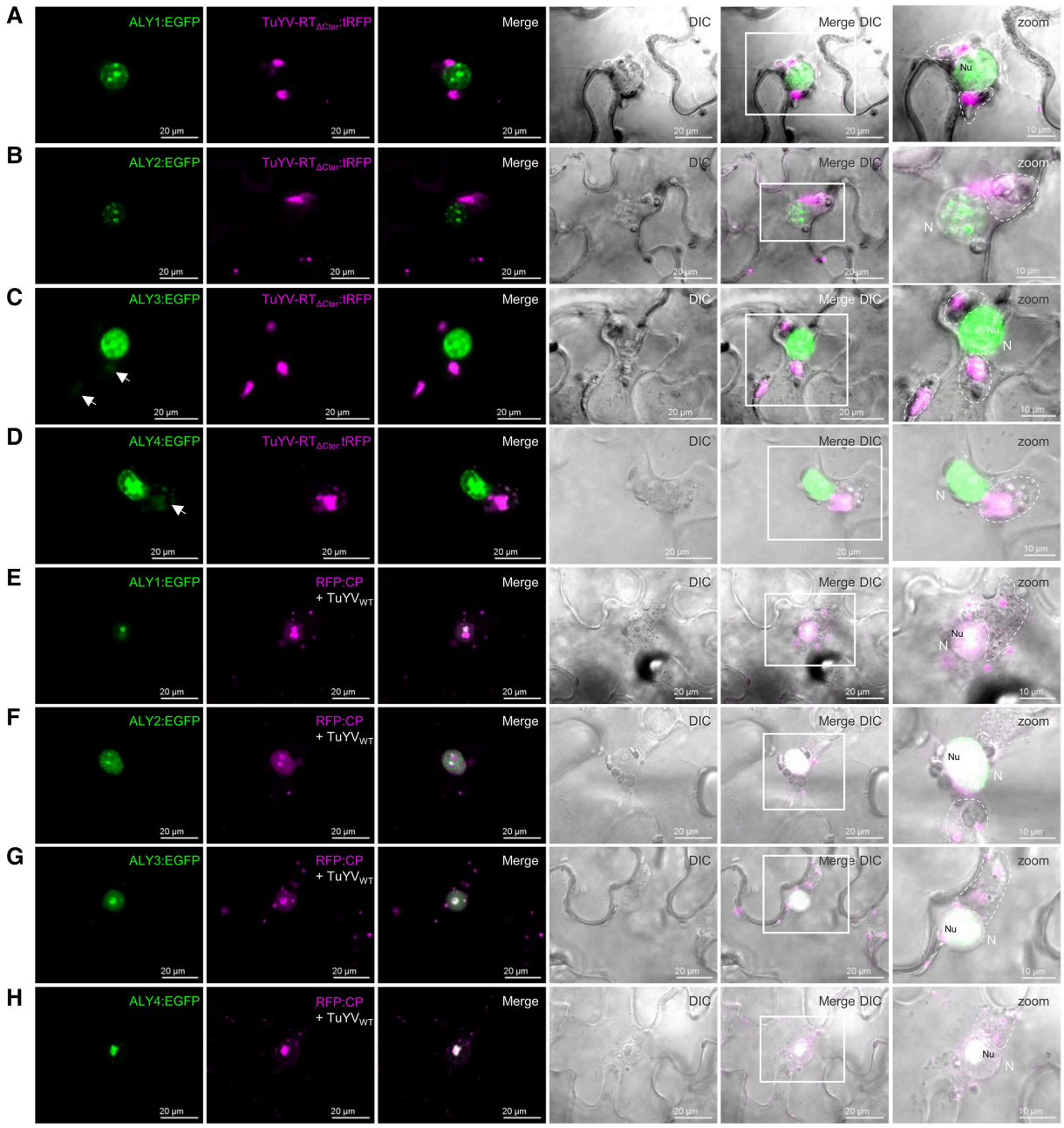

Figure 6. ALY:EGFP localization in *N. benthamiana* cells upon co-expression with TuYV. ALY1:EGFP, ALY2:EGFP, ALY3:EGFP, or ALY4:EGFP were, respectively, co-expressed either with TuYV-RT$_{\Delta Cter}$:tRFP **(A** to **D)** or with the RFP:CP protein and TuYV$_{WT}$ **(E** to **H)**. Leaf discs were analyzed 3 d post infiltration by LSCM. Perinuclear aggregates are marked by dotted circles in the last column. In **C** and **D**, the white arrows indicate the presence of a light green fluorescence of ALY3:EGFP and ALY4:EGFP outside of the nucleus (N). Enlargement of the structures surrounding the nucleus is shown on the right (zoom). $n = 2$, 4 leaf disks cut out in 2 or 3 leaves/plants, and 4 to 11 ROIs were analyzed/experimented. The scale bars represent 20 µm, and 10 µm for zoom. N, nucleus; Nu, nucleolus.

addition to its nuclear targeting, the RFP:RT protein was also observed along the cell periplasm in punctuated structures (Fig. 4A), a localization previously reported by Xu et al. (2018) for the PLRV GFP-RTP protein when expressed with the replicating PLRV. The punctuations along the cell wall colocalized with the plasmodesmata marker PDLP1 and the PLRV P17 movement protein (Xu et al. 2018). Interestingly, this specific localization was lost when the C-terminal domain of the TuYV RT protein was deleted in the TuYV-RT$_{\Delta Cter}$:tRFP clone (Fig. 5C). Consequently, these observations support the fact that the TuYV RT$_{Cter}$ domain is essential to target the viral protein to the plasma membrane. Finally, the plasma membrane localization of the RT protein could emphasize the critical role of the RT$_{Cter}$ domain in TuYV movement described by Rodriguez-Medina et al. (2015) through its ability to interact with the calcineurin B-like protein-interacting protein kinase-7, a protein localizing in or close to plasmodesmata and shown to regulate TuYV accumulation.

The co-expression of ALY proteins and either RFP:CP or RFP:RT proteins was accompanied by some spatial reorganization of the viral proteins in the nucleus, which were observed in speckles and foci formed by the ALY proteins when expressed alone. The RFP:CP conserved its nucleolar localization regardless of the ALY protein co-expressed (Fig. 3, B to E). Unexpectedly, the CP:RFP did not target the nucleolus when expressed alone

Downloaded from https://academic.oup.com/plphys/advance-article/doi/10.1093/plphys/kiae590/7920476 by guest on 12 December 2024

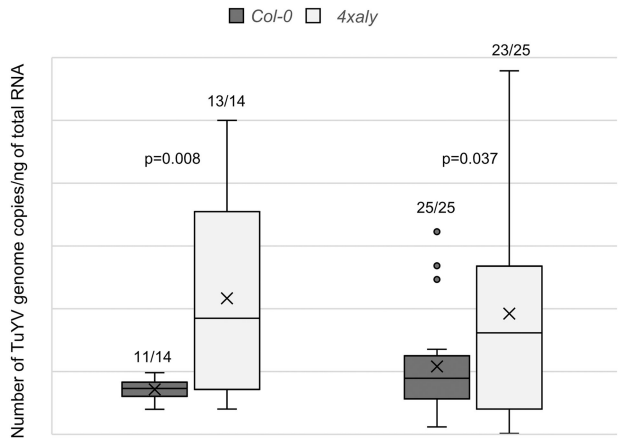

Figure 7. TuYV accumulation measured by RT-qPCR in *A. thaliana* Col-0 (dark grey boxes) and 4*xaly* mutant (light grey boxes) 2 wk after aphid inoculation. The box plots show the median (line), 25% to 75% percentiles (box), 10% to 90% percentiles (whisker), and outliers (dots). The ratio of infected plants/inoculated plants is indicated for each condition. An ANOVA test was performed to compare TuYV genome copy numbers in *A. thaliana* Col-0 and in the 4*xaly* mutant (*P*-value is indicated). Two independent experiments are shown (Experiments 1 and 2).

(Supplementary Fig. S5A) unlike the CP:GFP encoded by the PLRV, which is strongly nucleolar (Haupt et al. 2005). As TuYV CP:EGFP did not localise either in the nucleolus (Supplementary Fig. S9A), a plausible explanation could be that the C-terminally fluorescent tag induces steric hindrance or masks the NoLS target sequence, which loses its capacity to target the TuYV CP to the nucleolus. Nevertheless, the CP-RFP colocalized perfectly with the 4 ALY proteins in the nucleoplasm, which suggests a high affinity of the CP for all ALY proteins.

To investigate the localization of the ALY proteins in a viral infection context, we constructed 2 recombinant TuYV clones expressing slightly different shortened versions of the RT protein fused to the TagRFP. As no interaction was observed between any of the ALY proteins and the RT_{Cter} domain (at least in yeast), a large part of this domain was replaced by the fluorescent marker, resulting in labeled viruses with a genome size similar to that of the wild-type virus, thus limiting the risk of instability (Nurkiyanova et al. 2000; Bortolamiol-Bécet et al. 2018). When inoculated to *N. benthamiana* plants, both TuYV recombinant viruses developed a local infection and were able to move systemically, although their infection rate and titer were lower than those of the wild-type virus. These recombinant viruses enabled us to investigate the colocalization of ALY proteins with the viral-expressed RT in infiltrated cells.

The $RT_{\Delta Cter}$:tRFP proteins expressed by both recombinant TuYV viruses displayed localizations that greatly differed from those observed previously when the RFP:RT protein was expressed alone. First, the nuclear targeting of the RT protein was lost. This change in localization was unlikely due to the C-terminal deletion in the $RT_{\Delta Cter}$:tRFP as no nuclear targeting was detectable when the entire RFP-RT protein was expressed in the presence of $TuYV_{WT}$ (Supplementary Fig. S11). Similar observations were made with the PLRV full-length fluorescent RT protein expressed in infected cells (Haupt et al. 2005; Xu et al. 2018). RT nuclear localization may be hindered by interactions with viral partners or with host proteins recruited during infection. Conversely, the CP expressed in the presence of $TuYV_{WT}$ conserved its nuclear targeting and colocalized with each ALY:EGFP protein. Together with the interaction assays, these observations suggest that the CP is likely the major interactant of ALY proteins during viral infection.

TuYV produces perinuclear aggregates, potential viral factories

In this study, we show that TuYV infection induced large structures of different sizes localized in close proximity to the nucleus. A close observation of these structures suggests that they contain membranous-like material (see Fig. 5C for a particularly visible perinuclear structure in DIC). The presence of aggregates close to the nucleus were already reported in former studies by transmission electron microscopy (TEM) in tissues infected with the polerovirus beet western yellows virus (BWYV) in sugar beet (Esau and Hoefert 1972) and in PLRV-infected potato cells (Shepardson et al. 1980). We observed that these aggregates were partially but distinctly labeled with $RT_{\Delta Cter}$:tRFP but not clearly marked with the ALY:EGFP proteins when co-expressed with one of the fluorescent recombinant viruses. In a few cases, a weak EGFP signal produced by the ALY3:EGFP or ALY4:EGFP was detected outside of the nucleus in the viral-induced aggregates (Fig. 6, C and D, white arrows) and colocalized with the $RT_{\Delta Cter}$:tRFP. The presence of ALY3 and ALY4 outside of the nucleus could be either due to a fusion between the aggregates and the nuclear envelope, as reported by Esau and Hoefert (1972) and Shepardson et al. (1980), inducing nonspecific protein leakage from the nucleus to the aggregates or due to a real nuclear export, possibly through the interaction with the CP. The absence of colocalization of the $RT_{\Delta Cter}$:tRFP with ALY1:EGFP or ALY2:EGFP in the perinuclear structures could be explained by the presence of ALY1 and ALY2:EGFP signals below the detection threshold. Interestingly, the CP also displayed a localization in the viral-induced aggregates, supporting a possible role of these structures in virion assembly and/or intracellular movement (Laliberté and Zheng 2014; Wang 2015).

In their TEM studies, Esau and Hoefert (1972) and Shepardson et al. (1980) described fibrillar networks in the vesicles suggestive of nucleic acids. More recently, *N. benthamiana* cells infected with an unlabeled recombinant TuYV showed aggregates that could be labeled with the double-stranded RNA-binding domain of the B2 protein (Clavel et al. 2021), a marker of double-stranded RNA, and a signature of viral RNA replication (Monsion et al. 2018). These observations strongly identified these structures as the site of viral replication. In addition, Clavel et al. (2021) localized the main actors of the RNA silencing pathways (Yang and Li 2018), Dicer-like 2 (DCL2), Dicer-like 4 (DCL4), and ARGONAUTE 1, in or near these viral-induced aggregates, suggesting that these structures could also take part in antiviral RNAi-dependent immunity. Further investigations will be required to determine the contribution of the various viral and cellular factors present in the viral-induced structures to the different steps of the viral cycle.

CP-ALY protein interaction: a dual role in plant antiviral defense and viral manipulation?

Finally, to address the biological role of ALY proteins in the viral infection process, we investigated TuYV accumulation in *A. thaliana* mutants deficient in the expression of the 4 ALY genes. TuYV-infected quadruple 4*xaly* mutant plants exhibited a substantial increase in virus accumulation (2- to 3.3-fold according to the experiment). As the mutant develops severe phenotypic defects (Pfaff et al. 2018), the increase in viral titer could be attributed to a general enhanced susceptibility to any virus. The results obtained by Kubina et al. (2021) refute this hypothesis. They showed that the multiplication of the turnip mosaic virus, a potyvirus with a positive-sense RNA genome and a cytoplasmic replication cycle, as for the polerovirus TuYV, was not affected by the absence of expression of the 4 ALY genes. Conversely, infection by the CaMV,

Downloaded from https://academic.oup.com/plphys/advance-article/doi/10.1093/plphys/kiae590/7920476 by guest on 12 December 2024

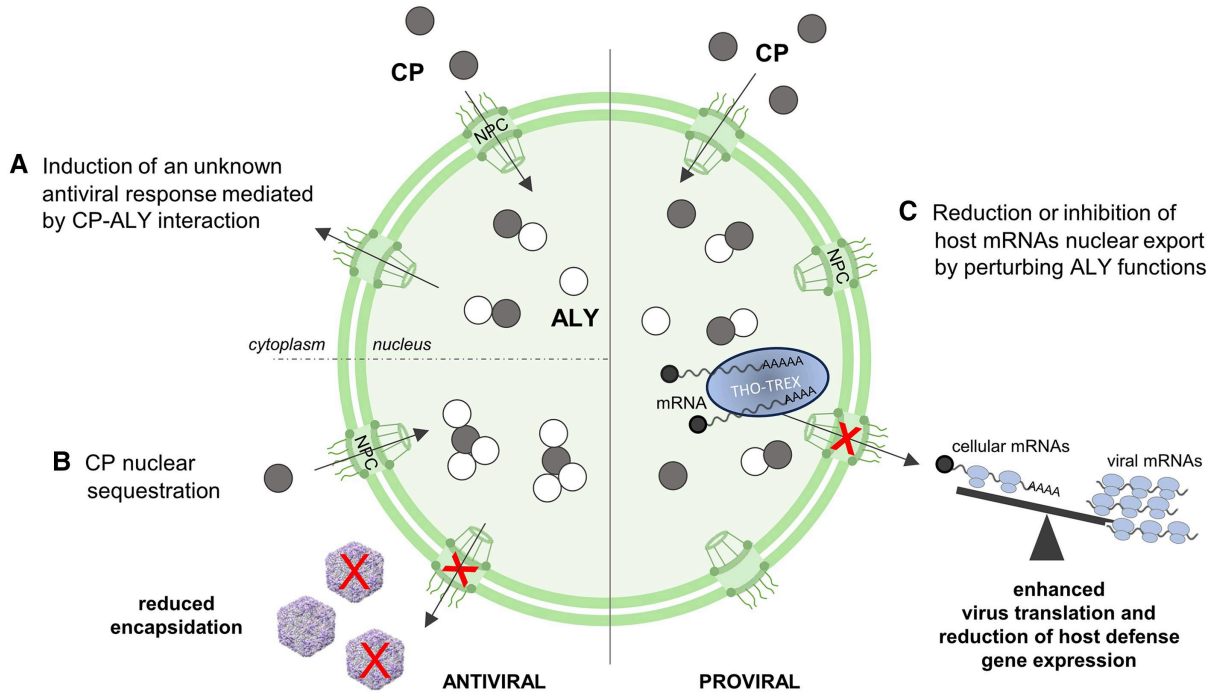

Figure 8. A working model of the possible impact of the CP-ALY interaction occurring in the nucleus upon TuYV infection leading to an antiviral or proviral effect. **A)** An unknown antiviral response mediated by CP-ALY interaction is triggered. **B)** The CP is sequestered in the nucleus, impeding its roles in the cytoplasm (encapsidation) and in the nucleus (recruitment of an unknown host factor leading to enhanced viral pathogenesis). **C)** Interaction of CP-ALY reduces or impairs the host mRNA nuclear export, leaving the translational machinery available for the viral RNAs, which could also inhibit specifically host defense gene expression. **A** and **B** are antiviral responses, while **C** denotes a proviral activity. A red cross indicates the blockage of the corresponding function. The CP and ALY are shown as dark grey and light grey circles, respectively. ALY represents any of the 4 ALY proteins. NPC, nuclear pore complex; THO-TREX, transcription-export (THO/TREX) protein complex.

which possesses a DNA genome and a nuclear replication cycle, was severely inhibited in this mutant (Kubina et al. 2021). The deficiency in the 4 ALY factors resulted in CaMV-partially resistant plants due to impaired viral pregenomic RNA export from the nucleus to the cytoplasm. The significant increase in TuYV accumulation in the 4*xaly* mutant could therefore endorse a role of ALY proteins in antiviral defense (Fig. 8A).

A similar observation was reported by Yang et al. (2020) in *N. benthamiana*. By reducing *via* RNA silencing the expression of NbALY617, the AtALY4 protein ortholog, they found higher titers of potato virus X (PVX). NbALY617 was shown to interact with P25, the pathogenicity factor of PVX, and participate in the regulation of pathogen-induced hypersensitive response by increasing the P25-triggered necrosis. Likewise, it was shown that the suppressor of RNA silencing P19 encoded by the tobacco bushy stunt virus could interact with other *N. benthamiana*-encoded ALY proteins, NbALY916 (initially referred to as Hin19, Park et al. 2004), NbALY617, and NbALY615, as well as with any of the 4 AtALY proteins (Uhrig et al. 2004). Interestingly, the co-expression of P19 and ALY1, ALY3, NbALY615, or NbALY1693 led to the relocalization of P19 from the cytoplasm to the nucleus, which subsequently compromised its RNA silencing suppression activity (Canto et al. 2006). Although the biological significance of the subcellular redistributions has not been further addressed upon viral infection, these results support the potential involvement of ALY proteins in antiviral defense. Moreover, the nuclear relocalization of P19 with only a subset of the ALY proteins tested, indicates specific or additional functions of these ALY proteins that become noticeable in the presence of the viral protein.

As neither the TuYV CP nor the RT protein are known to display some RNA silencing suppression activity, the antiviral activity of ALY proteins upon the inhibition of a viral suppressor activity is unlikely. A more plausible scenario could be the sequestration of the CP in the nucleoplasm after their interaction with ALY proteins, thus limiting the capsid protein's availability for the cytoplasmic process of genome encapsidation (Fig. 8B). As virions are essential for TuYV long-distance movement (Hipper et al. 2014), additional cytoplasmic CPs could partially explain the enhanced level of TuYV systemic accumulation in the *A. thaliana* quadruple mutant 4*xaly*. Such a strategy has been validated by the work carried out on the varicella-zoster virus (VZV) (Reichelt et al. 2011), in which a host antiviral defense was linked to nuclear sequestration of VZV nucleocapsids, which led to the inhibition of infectious VZV progeny formation. Finally, CP sequestration by ALY proteins could also prevent the recruitment of a yet unknown nuclear factor that could promote viral infection (Fig. 8B).

On the other hand, by entering into the nucleus and interacting with the ALY proteins, the CP could reduce or inhibit their role in the THO/TREX export complex, leading to a decrease of host mRNA nuclear export and expression, including potential host defense transcripts. In this scenario, the translational machinery would become more available for the viral mRNAs, thus supporting a proviral function of the ALY–CP interaction (Fig. 8C). This hypothesis is sustained by the data provided by Pfaff et al. (2018) showing that cellular mRNA nuclear export is reduced in this mutant. Similar situations have been reported previously for animal viruses, which developed various strategies that led to a functional inhibition or destruction of some specific nuclear factors and thereby impaired nuclear mRNA export. For instance, the NS1 protein of influenza virus A contributes to the blocking of the cellular mRNA export machinery *via* its multiple interactions with several exportins (Zhang et al. 2019). In the case of the poliovirus,

Downloaded from https://academic.oup.com/plphys/advance-article/doi/10.1093/plphys/kiae590/7920476 by guest on 12 December 2024

the 2A protease causes a degradation of 3 FG nucleoporins of the nuclear pore complex, perturbing the nucleo-cytoplasmic RNA and protein trafficking, which, in turn, leads to an altered expression of antiviral genes (Lizcano-Perret and Michiels 2021).

To conclude, we identified in this paper interactions between *A. thaliana* ALY adaptor proteins involved in the nuclear export of mRNAs and structural viral proteins of TuYV. Importantly, the absence of these proteins in the *Arabidopsis 4xaly* mutant led to a significant increase in TuYV accumulation in systemic tissues, suggesting that ALY proteins contribute to an antiviral defense mechanism or are the target of a manipulation strategy by TuYV to reduce the export of cellular mRNAs and thus promote its infection. It could be particularly relevant to analyze the behavior of plants overexpressing one or several ALY genes to observe a potential resistance on TuYV and other poleroviruses. The outcome of such experiments may provide opportunities to engineer antiviral resistances in agricultural crops.

Materials and methods

Virus inoculation by aphids and agrobacterium

Myzus persicae reared on *Capsicum annuum* were used for virus transmission experiments. A TuYV suspension was used at 50 ng/μL in an artificial medium (Bruyère et al. 1997). After a 24 h acquisition access period, 5 aphids were transferred per plant (Arabidopsis *4xaly* or Col-0) for virus inoculation. Three days later, aphids were eliminated using an insecticide treatment (Pirimor, Syngenta). Plants were infested with nonviruliferous aphids as a control. Agro-inoculations of *N. benthamiana* were performed as described by (Smirnova et al. 2015).

Yeast 2-hybrid experiments

A. thaliana ALY proteins were expressed from constructs described in Uhrig et al. (2004), TuYV CP and $RT_{\Delta Cter}$ proteins from pGBT9 and pGBKT7 vectors, respectively, reported in Mulot et al. (2018), and RT_{Cter} from pGBKT7 described in Rodriguez-Medina et al. (2015). A high-efficiency polyethylene glycol/lithium acetate-based method was used for preparing and transforming competent yeast cells. Y2HGold strain cells (Clontech) were grown in a 50 mL yeast extract–peptone–dextrose medium at 28 °C until the $OD_{600\ nm}$ reached 0.6. The cells were washed in sterile water and then in 100 mM lithium acetate in 10 mM Tris-HCl, 1 mM EDTA, pH 7.5 buffer (LiAc-TE). After centrifugation, the cells were resuspended in 250 μL of LiAc/TE buffer and 50 μL of these competent cells were used for each transformation as recommended by Clontech. Double-transformed yeast cells were selected on a minimal medium double dropout (a synthetic dextrose medium lacking tryptophan and leucine, SD/-WL). Three selected colonies were then plated on minimal medium quadruple dropouts (SD/-AHWL) containing aureobasidin A (Ozyme) (40 ng/mL). Experiments with the TuYV CP and RT_{Cter} were repeated twice and those with $RT_{\Delta Cter}$ 4 times with individual colonies.

Gene cloning and plasmid construction

All below-designated primers are listed in Supplementary Table S3. The TuYV RT ORF (nt 3,483 to 5,495) used in the co-immunoprecipitation experiments was cloned following a "megaprimer PCR" procedure. Two PCR fragments were generated using 2 couples of primers, 5′-Kpn-35Spro-dir and 3′-35Spro-omega-Nhe-CP-rev, and 5′-35Spro-omega-Nhe-CP-dir and RT-3′-Sal-Xba-rev, and a DNA template from plasmid pBW6.26 [where CP stop codon TAG is changed into TAC (Reutenauer et al. 1993)]. The resulting PCR fragments were then annealed and used for the synthesis of the large PCR fragment together with the primers 5′Kpn-35Spro-dir and RT-3′-Sal-Xba-rev. The PCR fragment was digested with *KpnI* and *XbaI* restriction enzymes, introduced into the plasmid pKS to generate pKS-35S:RT_{WT} and further inserted into the vector pBin61 to give rise to pBin35S:RT_{WT}. The latter was finally mobilized into *A. tumefaciens* GV3101.

The complete TuYV RT sequence was amplified from pKS-35S:RT_{WT} using primers 5′-CPRT-attB1-dir and 3′RT stop-attB2-rev and introduced into pDONR Zeo (Invitrogen) and further mobilized by Gateway technology into pH7WGR2 (VIB-Ugent Center for Plant Systems Biology) to obtain the RFP:RT fusion. The resulting plasmid pH7-RFP:RT was introduced into *A. tumefaciens* GV3101 for transient expression in *N. benthamiana*.

The ALY:EGFP constructions used for the subcellular localization analysis were obtained by reverse transcription and PCR amplification from *A. thaliana* Col-0 RNA using primers ALY1-5′ attB1-dir and ALY1-3′attB2-rev, ALY2-5′attB1-dir and ALY2-3′ attB2-rev, ALY3-5′attB1-dir and ALY3-3′attB2-rev, and ALY4-5′ attB1-dir and ALY4-3′attB2-rev. PCR fragments were mobilized into pDONR Zeo, followed by recombination into pH7FWG2. All clones were introduced in *A. tumefaciens* GV3101 for transient expression in *N. benthamiana*.

The TuYV CP sequence was introduced by restriction cloning into the pENTR4-CP using the primers 5′CP-Nco-dir, 3′-CP-Xba-stop-rev, and 3′-CP-Xba-nostop-rev. The CP sequence was further mobilized by Gateway cloning into pK7FWG2, pB7RWG2, pK7WGF2, and pB7WGR2 to generate pK7-CP:EGFP, pB7-CP:RFP, pK7-EGFP:CP, and pB7-RFP:CP, respectively. All Gateway clones were controlled by sequencing.

Two TuYV vectors encoding an RT protein fused to TagRFP were designed based on TuYV-RT_{GFP} construction (Boissinot et al. 2017). TuYV-$RT_{\Delta Cter}$:$tRFP_{fus}$ was built by Gibson Assembly cloning (Gibson et al. 2009) using 2 pairs of primers, RT-tRFP-dir and tRFP-RTfus-rev for the tRFP fragment and RT-tRFP-rev and tRFP-RTfus-dir to generate the viral vector backbone with pBW.A- (Leiser et al. 1992) as a template. In the resulting virus TuYV-$RT_{\Delta Cter}$:$tRFP_{fus}$, the RT protein was fused at the amino acid 489 to the TagRFP (tRFP) protein, which was kept in the frame with the RT last 8 amino acids. TuYV-RT:$tRFP_{stop}$ was similarly constructed using primers RT-tRFP-dir and tRFP-RTstop-rev to create a stop codon at the end of the TagRFP sequence. The following 24 nts viral sequence corresponding to the last 8 RT codons was retained. The viral vector backbone was generated using the primers RT-tRFP-rev and tRFP-RTstop-dir and the pBW.A- template. The corresponding plasmids pBS-TuYV-$RT_{\Delta Cter}$:$tRFP_{fus}$ and pBS-TuYV-$RT_{\Delta Cter}$:$tRFP_{stop}$ were controlled by sequencing. The viral-modified sequence was introduced into pBinTuYV$_{WT}$ by replacing the *SpeI-SalI* fragment (1,351 to 5,641) by the corresponding recombinant fragment. The plasmids pBinTuYV-$RT_{\Delta Cter}$:$tRFP_{fus}$ and pBinTuYV-$RT_{\Delta Cter}$:$tRFP_{stop}$ were finally introduced into *A. tumefaciens* GV3101 for agro-infection.

Transient protein expression in *N. benthamiana*

For fluorescence microscopy observations, co-immunoprecipitation, and western blot analyses, leaves of 5 wk-old *N. benthamiana* were infiltrated with *A. tumefaciens* prepared as described by (Smirnova et al. 2015). The bacteria containing plasmids of interest were infiltrated at an absorbance (OD_{600}) of 0.5, and 0.3 for the bacteria with the ALY:EGFP, VSR, and virus containing plasmids. Three days post infiltration, leaf discs were collected for confocal microscopy analysis. Samples for the western blot and

Downloaded from https://academic.oup.com/plphys/advance-article/doi/10.1093/plphys/kiae590/7920476 by guest on 12 December 2024

co-immunoprecipitation experiments were harvested and stored at −80 °C.

Optimization of ALY:GFP expression *in planta*

Vectors containing ALY1:GFP to ALY4:GFP were described by Uhrig et al. (2004). Four viral suppressors of RNA silencing (VSR) were tested to optimize ALY:GFP expression in *N. benthamiana*-infiltrated leaves: P0 of TuYV (Pazhouhandeh et al. 2006), P38 of the turnip crinkle virus (Thomas et al. 2003), Hc-Pro of the potato virus Y, and P19 of the tomato bushy stunt virus, Jay et al. (2023). Particular attention was paid to P19, which was shown to relocalize ALY2 and 4 from the nucleus to the cytoplasm (Uhrig et al. 2004). Based on the fluorescence observed by confocal microscopy when co-expressed with either AtALY proteins, we chose P38 to improve the expression of ALY1 and ALY2, P19 for ALY3, and P0 for ALY4 (Supplementary Fig. S2).

Co-immunoprecipitation experiments

The cell lysate was obtained by mechanical grinding of 1 g of *N. benthamiana* tissue in liquid nitrogen and subsequent addition of lysis buffer [Tris-HCl 50 mM pH 8, NaCl 50 mM, $MgCl_2$ 2 mM, DTT 1 mM, Triton X-100 1%, cOmplete EDTA-free Protease Inhibitor Cocktail (Roche)]. The samples were then clarified by 2 centrifugation steps at 14,000 rpm for 15 min at 4 °C, and anti-GFP µMACS magnetic beads (Miltenyi Biotech) were added to the supernatant and gently mixed for 45 min at 4 °C. The homogenates (input fractions) were loaded on a pre-equilibrated µ-column attached to a thermoMACS magnetic holder and washed 3 times with washing buffer (lysis buffer with 0,1% Triton X-100). Elution of the proteins was performed by adding 3 times 35 µL of elution buffer (Tris-HCl 50 mM pH 6.8, DTT 50 mM, EDTA 1 mM, SDS 1%, bromophenol blue 0,005%, glycerol 10%). Appropriate volumes of Laemmli x2 buffer (final concentration Tris-HCl 125 mM pH 6.8, Glycerol 5%, β-mercaptoethanol 5%, SDS 5%, Bromophenol Blue 0.005%) were added to the input samples and Laemmli x4 for the IP fractions before analysis by SDS-PAGE analysis.

Western blot analyses

The infiltrated *N. benthamiana* leaves (0.1 g) were dry-ground for 1 min at 10,000 rpm with glass beads (1.7 to 2 mm) in the Homogenizer tissue grinder Precellys Evolution. Four hundred microliters of lysis buffer (see above) were added before using a new grinding cycle of 1 min at 10,000 rpm. After centrifugation for 3 min at 3,000 rpm, the protein concentration of the supernatant was determined by using a Bradford assay (Bio-Rad). Appropriate volumes of Laemmli buffer X2 were added to the samples and heated at 95 °C for 5 min before performing centrifugation for 3 min at 3,000 rpm. Eighty micrograms of total proteins were loaded on a 10% or 12% SDS-PAGE, except when indicated.

For RFP:CP samples, urea extraction was performed to improve the process of protein detection. One hundred milligrams of infiltrated leaves were dry-ground with glass beads for 30 s using a Silamat S6 shaker (Ivoclar) before adding 200 µL of 8 M urea and using a further 30 s grinding cycle. A suitable volume of Laemmli x4 buffer was then added before heating at 95 °C for 10 min and centrifugation for 5 min at 10,000 rpm.

Blotted nitrocellulose membranes (Immobilon-P, Millipore) were incubated with rabbit antibodies against either the GFP (produced by D. Scheidecker), RFP (ChromoTek), TuYV CP, or RT protein (Reutenauer et al. 1993). Immunoblots were further incubated with goat antirabbit antibodies (or goat antimouse antibodies for blots previously incubated with anti-RFP antibodies) coupled to peroxidase and visualized using chemiluminescence according to the manufacturer's instructions (Clarity Max, Bio-Rad). Pictures were taken using the imaging system Fusion FX Vilber.

Protoplast infection experiments

The preparation and transfection of *A. thaliana* protoplasts were carried out according to the protocol laid down by Lalande et al. (2020). Twenty-four hours after transfection with the viral constructs pBS-TuYV-$RT_{\Delta Cter}$:$tRFP_{fus}$ or pBS-TuYV-$RT_{\Delta Cter}$:$tRFP_{stop}$ and/or pCK-EGFP plasmid control, the protoplasts were deposited between the slide and the coverslip in Secure-Seal Spacer for visualization under LSCM LSM780 (Zeiss, France).

Epifluorescence and confocal laser scanning microscopy

Hand-cut cross sections of petioles and roots were mounted in water. TagRFP fluorescence was observed using an Axio Imager M2 microscope (Zeiss, France) equipped with a Hamamatsu digital camera. Observations were performed on noninoculated leaves and roots of infected *N. benthamiana* 3 wk post infection.

Agro-infiltrated *N. benthamiana* leaf discs were observed using a 40× oil-immersion objective (numerical aperture of 1.4) with an LSM780 microscope (Zeiss). Confocal acquisitions were performed with detection wavelength windows of 493 to 598 nm for the EGFP and 582 to 617 nm for the TagRFP and RFP. All images were collected separately to minimalize bleed-through. The detection range was optimized for each fluorophore to reduce the chloroplast's autofluorescence. The images were then processed using ImageJ and the plugin FigureJ (Collins 2007). For each condition, observations by confocal microscopy were performed at least twice, and the number of images analyzed was indicated in the legend of each figure.

Virus detection in plants by DAS-ELISA and RT-qPCR and virus progeny analysis

TuYV-$RT_{\Delta Cter}$:tRFP mutant detection in noninoculated leaves of *N. benthamiana* after agro-infiltration was performed by DAS-ELISA using TYV-specific antibodies (Loewe, Germany) as described by Bruyère et al. (1997). TuYV accumulation in *A. thaliana* Col-0 and *4xaly* mutants was analyzed by RT-qPCR. One hundred mg of tissue was collected 2 wk post inoculation and ground in a mortar with liquid nitrogen. Total RNA was extracted with the NucleoSpin RNA plant (Macherey-Nagel). Viral RNA was reverse-transcribed and PCR-amplified as described by Mulot et al. (2018). To determine the copy number of the TuYV genome in the infected plants, a standard curve ranging from 1.10^8 to 1.10^3 ng/µL was obtained from TuYV RNA extracted from purified virions (Mulot et al. 2018). The viral progeny in the *N. benthamiana* plants inoculated with the TuYV-$RT_{\Delta Cter}$:tRFP mutants was analyzed by RT-PCR following the protocol described in Boissinot et al. (2017).

RT-qPCR analysis of ALY gene expression

Total plant RNA was extracted 2 wk after inoculation by aphids (viruliferous or nonviruliferous). Plant samples (5 noninfected and 5 TuYV-infected) were ground in liquid nitrogen and RNA extraction was performed using the NucleoSpin RNA plant kit followed by DNase treatment (Macherey-Nagel). Reverse transcription (RT) was performed on 1 µg of RNA with 1 µL of an oligo

Downloaded from https://academic.oup.com/plphys/advance-article/doi/10.1093/plphys/kiae590/7920476 by guest on 12 December 2024

dT(15) primer with M-MLV reverse transcriptase (Promega) in 20 µL. Two microliters of cDNA were used for quantitative PCR with Evagreen mastermix (Biorad) in a total of 10 µL. Five couples of primers were tested in order to select the best reference genes with Normfinder (Andersen et al. 2004) and Bestkeepers (Pfaffl et al. 2004) programs. Three reference genes [*RHIP1* (AT4G26410); *GAPDH* (AT1G13440); *EF1α* (AT5G60390)] were selected. Specific primers were used for each ALY gene and PCR efficiencies were assessed on a cDNA serial of 5-fold dilutions. An internal sample control was used to compare the results obtained from the different PCR plates. The relative *aly* gene expression (ER) was analyzed according to the formula

$$ER = \frac{E_{gi}^{(Ct_{control} - Ct_{gi})}}{\sqrt[f]{\prod_{o}^{f} E_{ref_o}^{(Ct_{control} - Ct_{ref_o})}}}$$

described by (Hellemans et al. 2007). The relative expressions of ALY1, ALY2, and ALY3 genes were statistically analyzed using an ANOVA test. For the ALY4 relative expression analysis, a Kruskall–Wallis test was performed because of variance heterogeneity.

Accession numbers

Sequence data from this article can be found in the GenBank/EMBL data libraries under the following accession numbers: TuYV (former BWYV-FL1): NC_003743.1; AtALY1: AT5G55950; AtALY2: AT5G02530.1; AtALY3: AT1G66260.1; AtALY4: AT5G37720.1.

Acknowledgments

We are grateful to Dr Stuart Mac Farlane for his gift of the AtALY1, AtALY2, AtALY3, and AtALY4 clones and the *Arabidopsis aly* SALK and RNAi mutants, to Dr Klaus D. Grasser for the 4*xaly* knock-out mutant, and to Julia de Cilia for the pENTR4-CP clone. Maria Dimitrova and Corinne Schmitt-Keichinger are warmly acknowledged for their critical reading of the manuscript. The authors would like to thank Jon Pol Gales for his help in producing and infecting *Arabidopsis* protoplasts and Marie-Edith Chabouté for her advice on specific fluorescent subcellular markers. Quentin Chesnais is thanked for his assistance in the statistical tests.

Author contributions

S.B., D.K., V.B., and V.Z.-G. designed the research; D.K., S.B., C.P., D.S., and C.V. performed the experiments; D.K., S.B., V.B., and V.Z.-G. analyzed the data and wrote the paper; D.G. contributed to the interpretation of the results and corrected the manuscript.

Supplementary data

The following materials are available in the online version of this article.

Supplementary Figure S1. Autoactivation tests of co-transformed yeasts.

Supplementary Figure S2. Estimation of abundance of ALY:GFP proteins co-expressed with different viral RNA silencing suppressors.

Supplementary Figure S3. Interaction assays of CP and RT proteins expressed in TuYV-infected leaves with each of the 4 ALY:GFP proteins.

Supplementary Figure S4. Subcellular localization of the 4 ALY:EGFP proteins.

Supplementary Figure S5. Subcellular colocalization analysis of the ALY:EGFP proteins upon their co-expression with the CP:RFP protein.

Supplementary Figure S6. Immunodetection of ALY:EGFP proteins and viral proteins in agro-infiltrated *N. benthamiana* leaves.

Supplementary Figure S7. Infectivity analysis of 2 TuYV recombinant clones expressing the $RT_{\Delta Cter}$ protein tagged with the tRFP.

Supplementary Figure S8. Detection of the viral-induced perinuclear aggregates and localization of various fluorescent control proteins.

Supplementary Figure S9. Confocal imaging of CP:EGFP and EGFP:CP localization with and without TuYV.

Supplementary Figure S10. Relative expressions of *ALY1*, *ALY2*, *ALY3*, and *ALY4* genes in *A. thaliana* Col-0 2 wk after TuYV inoculation by aphids.

Supplementary Figure S11. Subcellular localization analysis of RFP:RT protein upon its co-expression with $TuYV_{WT}$.

Supplementary Table S1. Analysis of TuYV-$RT_{\Delta Cter}$:tRFP mutant accumulation by DAS-ELISA in systemic leaves of *N. benthamiana* 3 wk post infection.

Supplementary Table S2. Analysis of TuYV accumulation in noninoculated leaves of *A. thaliana* Col-0 and single *aly* mutants.

Supplementary Table S3. List of the primers used.

Funding

D.K. was supported by a fellowship from the Ministère de l'Enseignement Supérieur et de la Recherche and from the Université de Strasbourg. This research was partly supported by the French National Research Agency for research (ANR n°ANR-20-CE35-010). Funding for publication costs is covered by the institut de biologie moléculaire des plantes (CNRS) and the INRAE Grand Est Colmar.

Conflict of interest statement. None declared.

Data availability

The data underlying this article are available in the article and in its online supplementary material.

References

Andersen CL, Jensen JL, Ørntoft TF. Normalization of real-time quantitative reverse transcription-PCR data: a model-based variance estimation approach to identify genes suited for normalization, applied to bladder and colon cancer data sets. *Cancer Res*. 2004:64 (15):5245–5250. https://doi.org/10.1158/0008-5472.CAN-04-0496

Boissinot S, Erdinger M, Monsion B, Ziegler-Graff V, Brault V. Both structural and non-structural forms of the readthrough protein of cucurbit aphid-borne yellows virus are essential for efficient systemic infection of plants. *PLoS One*. 2014:9(4):e93448. https://doi.org/10.1371/journal.pone.0093448

Boissinot S, Pichon E, Sorin C, Piccini C, Scheidecker D, Ziegler-Graff V, Brault V. Systemic propagation of a fluorescent infectious clone of a polerovirus following inoculation by agrobacteria and aphids. *Viruses*. 2017:9(7):166. https://doi.org/10.3390/v9070166

Bortolamiol-Bécet D, Monsion B, Chapuis S, Hleibieh K, Scheidecker D, Alioua A, Bogaert F, Revers F, Brault V, Ziegler-Graff V. Phloem-triggered virus-induced gene silencing using a recombinant polerovirus. *Front Microbiol*. 2018:9:2449. https://doi.org/10.3389/fmicb.2018.02449

Brault V, van den Heuvel JF, Verbeek M, Ziegler-Graff V, Reutenauer A, Herrbach E, Garaud JC, Guilley H, Richards K, Jonard G, *et al.*

Downloaded from https://academic.oup.com/plphys/advance-article/doi/10.1093/plphys/kiae590/7920476 by guest on 12 December 2024

Aphid transmission of beet western yellows luteovirus requires the minor capsid read-through protein P74. *EMBO J*. 1995:14(4): 650–659. https://doi.org/10.1002/j.1460-2075.1995.tb07043.x

Brice AM, Watts E, Hirst B, Jans DA, Ito N, Moseley GW. Implication of the nuclear trafficking of rabies virus P3 protein in viral pathogenicity. *Traffic*. 2021:22(12):482–489. https://doi.org/10.1111/tra.12821

Bruyère A, Brault V, Ziegler-Graff V, Simonis M-TT, Van Den Heuvel JFJM, Richards K, Guilley H, Jonard G, Herrbach E. Effects of mutations in the beet western yellows virus readthrough protein on its expression and packaging and on virus accumulation, symptoms, and aphid transmission. *Virology*. 1997:230(2): 323–334. https://doi.org/10.1006/viro.1997.8476

Canto T, Uhrig JF, Swanson M, Wright KM, MacFarlane SA. Translocation of Tomato bushy stunt virus P19 protein into the nucleus by ALY proteins compromises its silencing suppressor activity. *J Virol*. 2006:80(18):9064–9072. https://doi.org/10.1128/JVI.00953-06

Chi B, Wang Q, Wu G, Tan M, Wang L, Shi M, Chang X, Cheng H. Aly and THO are required for assembly of the human TREX complex and association of TREX components with the spliced mRNA. *Nucleic Acids Res*. 2013:41(2):1294–1306. https://doi.org/10.1093/nar/gks1188

Clavel M, Lechner E, Incarbone M, Vincent T, Cognat V, Smirnova E, Lecorbeiller M, Brault V, Ziegler-Graff V, Genschik P. Atypical molecular features of RNA silencing against the phloem-restricted polerovirus TuYV. *Nucleic Acids Res*. 2021:49(19):11274–11293. https://doi.org/10.1093/nar/gkab802

Collins TJ. Imagej for microscopy. *BioTechniques*. 2007:43(1 Suppl): 25–30. https://doi.org/10.2144/000112517

D'Arcy CJ, Domier LL. Family luteoviridae. In: Fauquet CM, Mayo MA, Maniloff J, Desselberger U, Ball LA, editors. *Virus taxonomy. Eighth report of the international committee on taxonomy of viruses*. San Diego (CA): Elsevier; 2005a. p. 891–900.

D'Arcy CJ, Domier LL. *Barley yellow dwarf*. APS, Vol. 5. St Paul, USA: The Plant Health Instructor; 2005b https://doi.org/10.1094/PHI-I-2000-1103-01

Delfosse VC, Barrios Barón MP, Distéfano AJ. What we know about poleroviruses: advances in understanding the functions of polerovirus proteins. *Plant Pathol*. 2021:70(5):1047–1061. https://doi.org/10.1111/ppa.13368

Dodds PN, Rathjen JP. Plant immunity: towards an integrated view of plant-pathogen interactions. *Nat Rev Genet*. 2010:11(8):539–548. https://doi.org/10.1038/nrg2812

Edwards MC, Fetch TG, Schwarz PB, Steffenson BJ. Effect of *Barley yellow dwarf virus* infection on yield and malting quality of barley. *Plant Dis*. 2001:85(2):202–207. https://doi.org/10.1094/PDIS.2001.85.2.202

Ehrnsberger HF, Grasser M, Grasser KD. Nucleocytosolic mRNA transport in plants: export factors and their influence on growth and development. *J Exp Bot*. 2019:70(15):3757–3763. https://doi.org/10.1093/jxb/erz173

Esau K, Hoefert LL. Ultrastructure of sugarbeet leaves infected with beet western yellows virus. *J Ultrastruct Res*. 1972:40(5–6): 556–571. https://doi.org/10.1016/S0022-5320(72)80043-1

Filichkin SA, Lister RM, McGrath PF, Young MJ. In vivo expression and mutational analysis of the barley yellow dwarf virus readthrough gene. *Virology*. 1994:205(1):290–299. https://doi.org/10.1006/viro.1994.1645

Gales JP, Kubina J, Geldreich A, Dimitrova M. Strength in diversity: nuclear export of viral RNAs. *Viruses*. 2020:12(9):1014. https://doi.org/10.3390/v12091014

Garcia-Ruiz H. Susceptibility genes to plant viruses. *Viruses*. 2018:10(9):484. https://doi.org/10.3390/v10090484

Gibson DG, Young L, Chuang R-Y, Venter JC, Hutchison CA, Smith HO. Enzymatic assembly of DNA molecules up to several hundred kilobases. *Nat Methods*. 2009:6(5):343–345. https://doi.org/10.1038/nmeth.1318

Haupt S, Stroganova T, Ryabov E, Kim SH, Fraser G, Duncan G, Mayo MA, Barker H, Taliansky M. Nucleolar localization of potato leafroll virus capsid proteins. *J Gen Virol*. 2005:86(10):2891–2896. https://doi.org/10.1099/vir.0.81101-0

Heath CG, Viphakone N, Wilson SA. The role of TREX in gene expression and disease. *Biochem J*. 2016:473(19):2911–2935. https://doi.org/10.1042/BCJ20160010

Hellemans J, Mortier G, De Paepe A, Speleman F, Vandesompele J. Qbase relative quantification framework and software for management and automated analysis of real-time quantitative PCR data. *Genome Biol*. 2007:8(2):R19. https://doi.org/10.1186/gb-2007-8-2-r19

Hipper C, Monsion B, Bortolamiol-Bécet D, Ziegler-Graff V, Brault V. Formation of virions is strictly required for turnip yellows virus long-distance movement in plants. *J Gen Virol*. 2014:95(2): 496–505. https://doi.org/10.1099/vir.0.058867-0

Hossain R, Menzel W, Lachmann C, Varrelmann M. New insights into virus yellows distribution in Europe and effects of beet yellows virus, beet mild yellowing virus, and beet chlorosis virus on sugar beet yield following field inoculation. *Plant Pathol*. 2021:70(3): 584–593. https://doi.org/10.1111/ppa.13306

Hu B, Yu L, Zhu N, Xie J. Cellular UAP56 interacts with the HBx protein of the hepatitis B virus and is involved in viral RNA nuclear export in hepatocytes. *Exp Cell Res*. 2020:390(1):111929. https://doi.org/10.1016/j.yexcr.2020.111929

Jay F, Brioudes F, Voinnet O. A contemporary reassessment of the enhanced transient expression system based on the tombusviral silencing suppressor protein P19. *Plant J*. 2023:113(1):186–204. https://doi.org/10.1111/tpj.16032

Jin L, Chen M, Xiang M, Guo Z. RNAi-based antiviral innate immunity in plants. *Viruses*. 2022:14(2):432. https://doi.org/10.3390/v14020432

Jones RAC, Coutts BA, Hawkes J. Yield-limiting potential of Beet western yellows virus in Brassica napus. *Aust J Agric Res*. 2007:58(8): 788. https://doi.org/10.1071/AR06391

Kang Y, Cullen BR. The human Tap protein is a nuclear mRNA export factor that contains novel RNA-binding and nucleocytoplasmic transport sequences. *Genes Dev*. 1999:13(9):1126–1139. https://doi.org/10.1101/gad.13.9.1126

Kubina J, Geldreich A, Gales JP, Baumberger N, Bouton C, Ryabova LA, Grasser KD, Keller M, Dimitrova M. Nuclear export of plant pararetrovirus mRNAs involves the TREX complex, two viral proteins and the highly structured 5′ leader region. *Nucleic Acids Res*. 2021:49(15):8900–8922. https://doi.org/10.1093/nar/gkab653

Kushwaha NK, Hafrén A, Hofius D. Microreview autophagy—virus interplay in plants : from antiviral recognition to proviral manipulation. *Mol Plant Pathol*. 2019:20(9):1211–1216. https://doi.org/10.1111/mpp.12852

Lalande S, Chery M, Ubrig E, Hummel G, Kubina J, Geldreich A, Drouard L. Transfection of small noncoding RNAs into *Arabidopsis thaliana* protoplasts. *Methods Mol Biol*. 2020:2166: 413–429. https://doi.org/10.1007/978-1-0716-0712-1_24

Laliberté J-F, Zheng H. Viral manipulation of plant host membranes. *Annu Rev Virol*. 2014:1(1):237–259. https://doi.org/10.1146/annurev-virology-031413-085532

Leiser RM, Ziegler-Graff V, Reutenauer A, Herrbach E, Lemaire O, Guilley H, Richards K, Jonard G. Agroinfection as an alternative to insects for infecting plants with beet western yellows luteovirus. *Proc Natl Acad Sci U S A*. 1992:89(19):9136–9140. https://doi.org/10.1073/pnas.89.19.9136

Downloaded from https://academic.oup.com/plphys/advance-article/doi/10.1093/plphys/kiae590/7920476 by guest on 12 December 2024

Lizcano-Perret B, Michiels T. Nucleocytoplasmic trafficking perturbation induced by picornaviruses. *Viruses*. 2021:13(7):1210. https://doi.org/10.3390/v13071210

Maio F, Helderman TA, Arroyo-Mateos M, Van Der Wolf M, Boeren S, Prins M, van den Burg HA. Identification of tomato proteins that interact with replication initiator protein (Rep) of the geminivirus TYLCV. *Front Plant Sci*. 2020:11:1069. https://doi.org/10.3389/fpls.2020.01069

Masuda S, Das R, Cheng H, Hurt E, Dorman N, Reed R. Recruitment of the human TREX complex to mRNA during splicing. *Genes Dev*. 2005:19(13):1512–1517. https://doi.org/10.1101/gad.1302205

Monsion B, Incarbone M, Hleibieh K, Poignavent V, Ghannam A, Dunoyer P, Daeffler L, Tilsner J, Ritzenthaler C. Efficient detection of long dsRNA in vitro and in vivo using the dsRNA binding domain from FHV B2 protein. *Front Plant Sci*. 2018:9:70. https://doi.org/10.3389/fpls.2018.00070

Mulot M, Boissinot S, Monsion B, Rastegar M, Clavijo G, Halter D, Bochet N, Erdinger M, Brault V. Comparative analysis of RNAi-based methods to down-regulate expression of two genes expressed at different levels in *Myzus persicae*. *Viruses*. 2016:8(11):316. https://doi.org/10.3390/v8110316

Mulot M, Monsion B, Boissinot S, Rastegar M, Meyer S, Bochet N, Brault V. Transmission of *Turnip yellows virus* by *Myzus persicae* is reduced by feeding aphids on double-stranded RNA targeting the ephrin receptor protein. *Front Microbiol*. 2018:9:457. https://doi.org/10.3389/fmicb.2018.00457

Mutterer JD, Stussi-Garaud C, Michler P, Richards KE, Jonard G, Ziegler-Graff V. Role of the beet western yellows virus readthrough protein in virus movement in Nicotiana clevelandii. *J Gen Virol*. 1999:80(10):2771–2778. https://doi.org/10.1099/0022-1317-80-10-2771

Nicaise V. Lost in translation: an antiviral plant defense mechanism revealed. *Cell Host Microbe*. 2015:17(4):417–419. https://doi.org/10.1016/j.chom.2015.03.009

Nurkiyanova KM, Ryabov EV, Commandeur U, Duncan GH, Canto T, Gray SM, Mayo MA, Taliansky ME. Tagging potato leafroll virus with the jellyfish green fluorescent protein gene. *J Gen Virol*. 2000:81(3):617–626. https://doi.org/10.1099/0022-1317-81-3-617

Park J-W, Faure-Rabasse S, Robinson MA, Desvoyes B, Scholthof HB. The multifunctional plant viral suppressor of gene silencing P19 interacts with itself and an RNA binding host protein. *Virology*. 2004:323(1):49–58. https://doi.org/10.1016/j.virol.2004.02.008

Pazhouhandeh M, Dieterle M, Marrocco K, Lechner E, Berry B, Brault V, Hemmer O, Kretsch T, Richards KE, Genschik P, *et al*. F-box-like domain in the polerovirus protein P0 is required for silencing suppressor function. *Proc Natl Acad Sci U S A*. 2006:103(6):1994–1999. https://doi.org/10.1073/pnas.0510784103

Peter KA, Gildow F, Palukaitis P, Gray SM. The C terminus of the polerovirus p5 readthrough domain limits virus infection to the phloem. *J Virol*. 2009:83(11):5419–5429. https://doi.org/10.1128/JVI.02312-08

Peter KA, Liang D, Palukaitis P, Gray SM. Small deletions in the potato leafroll virus readthrough protein affect particle morphology, aphid transmission, virus movement and accumulation. *J Gen Virol*. 2008:89(8):2037–2045. https://doi.org/10.1099/vir.0.83625-0

Pfaff C, Ehrnsberger HF, Flores-Tornero M, Sørensen BB, Schubert T, Längst G, Griesenbeck J, Sprunck S, Grasser M, Grasser KD. ALY RNA-binding proteins are required for nucleocytosolic mRNA transport and modulate plant growth and development. *Plant Physiol*. 2018:177(1):226–240. https://doi.org/10.1104/PP.18.00173

Pfaffl MW, Tichopad A, Prgomet C, Neuvians TP. Determination of stable housekeeping genes, differentially regulated target genes and sample integrity: BestKeeper—excel-based tool using pairwise correlations. *Biotechnol Lett*. 2004:26(6):509–515. https://doi.org/10.1023/B:BILE.0000019559.84305.47

Reichelt M, Wang L, Sommer M, Perrino J, Nour AM, Sen N, Baiker A, Zerboni L, Arvin AM. Entrapment of viral capsids in nuclear PML cages is an intrinsic antiviral host defense against varicella-zoster virus. *PLoS Pathog*. 2011:7(2):e1001266. https://doi.org/10.1371/journal.ppat.1001266

Reutenauer A, Ziegler-Graff V, Lot H, Scheidecker D, Guilley H, Richards K, Jonard G. Identification of beet western yellows luteovirus genes implicated in viral replication and particle morphogenesis. *Virology*. 1993:195(2):692–699. https://doi.org/10.1006/viro.1993.1420

Revollon S, Strub JM, Fitchette A-C, Wiss L, Gomord V, Van Dorsselaer A, Brault V. A reinvestigation provides no evidence for sugar residues on structural proteins of poleroviruses and argues against a role for glycosylation of virus structural proteins in aphid transmission. *Virology*. 2010:402(2):303–314. https://doi.org/10.1016/j.virol.2010.03.037

Rodriguez-Medina C, Boissinot S, Chapuis S, Gereige D, Rastegar M, Erdinger M, Revers F, Ziegler-Graff V, Brault V. A protein kinase binds the C-terminal domain of the readthrough protein of Turnip yellows virus and regulates virus accumulation. *Virology*. 2015:486:44–53. https://doi.org/10.1016/j.virol.2015.08.031

Rodriguez-Peña R, Mounadi KE, Garcia-Ruiz H. Changes in subcellular localization of host proteins induced by plant viruses. *Viruses*. 2021:13(4):677. https://doi.org/10.3390/v13040677

Shepardson S, Esau K, McCrum R. Ultrastructure of potato leaf phloem infected with potato leafroll virus. *Virology*. 1980:105(2):379–392. doi:0042-6822(80)90039-2

Smirnova E, Firth AE, Miller WA, Scheidecker D, Brault V, Reinbold C, Rakotondrafara AM, Chung BY-W, Ziegler-Graff V. Discovery of a small non-AUG-initiated ORF in poleroviruses and luteoviruses that is required for long-distance movement. *PLoS Pathog*. 2015:11(5):e1004868. https://doi.org/10.1371/journal.ppat.1004868

Stewart M. Polyadenylation and nuclear export of mRNAs. *J Biol Chem*. 2019:294(9):2977–2987. https://doi.org/10.1074/jbc.REV118.005594

Tessier TM, Dodge MJ, Prusinkiewicz MA, Mymryk JS. Viral appropriation: laying claim to host nuclear transport machinery. *Cells*. 2019:8(6):559. https://doi.org/10.3390/cells8060559

Thomas CL, Leh V, Lederer C, Maule AJ. Turnip crinkle virus coat protein mediates suppression of RNA silencing in *Nicotiana benthamiana*. *Virology*. 2003:306(1):33–41. https://doi.org/10.1016/S0042-6822(02)00018-1

Tian X, Devi-Rao G, Golovanov AP, Sandri-Goldin RM. The interaction of the cellular export adaptor protein Aly/REF with ICP27 contributes to the efficiency of herpes simplex virus 1 mRNA export. *J Virol*. 2013:87(13):7210–7217. https://doi.org/10.1128/jvi.00738-13

Uhrig JF, Canto T, Marshall D, MacFarlane SA. Relocalization of nuclear ALY proteins to the cytoplasm by the tomato bushy stunt virus P19 pathogenicity protein. *Plant Physiol*. 2004:135(4):2411–2423. https://doi.org/10.1104/pp.104.046086

Viphakone N, Hautbergue GM, Walsh M, Chang C-T, Holland A, Folco EG, Reed R, Wilson SA. TREX exposes the RNA-binding domain of Nxf1 to enable mRNA export. *Nat Commun*. 2012:3(1):1006. https://doi.org/10.1038/ncomms2005

Wang A. Dissecting the molecular network of virus-plant interactions: the complex roles of host factors. *Annu Rev Phytopathol*. 2015:53(1):45–66. https://doi.org/10.1146/annurev-phyto-080614-120001

Wu X, Valli A, García JA, Zhou X, Cheng X. The Tug-of-War between plants and viruses: great progress and many remaining questions. *Viruses*. 2019:11(3):203. https://doi.org/10.3390/v11030203

Xu Y, Da Silva WL, Qian Y, Gray SM. An aromatic amino acid and associated helix in the C-terminus of the potato leafroll virus minor

Downloaded from https://academic.oup.com/plphys/advance-article/doi/10.1093/plphys/kiae590/7920476 by guest on 12 December 2024

capsid protein regulate systemic infection and symptom expression. *PLoS Pathog*. 2018:14(11):e1007451. https://doi.org/10.1371/journal.ppat.1007451

Yang X, Tian Y, Zhao X, Jiang L, Chen Y, Hu S, MacFarlane S, Chen J, Lu Y, Yan F. NbALY916 is involved in potato virus X P25-triggered cell death in *Nicotiana benthamiana*. *Mol Plant Pathol*. 2020:21(11):1495–1501. https://doi.org/10.1111/mpp.12986

Yang Z, Li Y. Dissection of RNAi-based antiviral immunity in plants. *Curr Opin Virol*. 2018:32:88–99. https://doi.org/10.1016/j.coviro.2018.08.003

Zhang K, Xie Y, Muñoz-Moreno R, Wang J, Zhang L, Esparza M, García-Sastre A, Fontoura BMA, Ren Y. Structural basis for influenza virus NS1 protein block of mRNA nuclear export. *Nat Microbiol*. 2019:4(10):1671–1679. https://doi.org/10.1038/s41564-019-0482-x

Downloaded from https://academic.oup.com/plphys/advance-article/doi/10.1093/plphys/kiae590/7920476 by guest on 12 December 2024